Postprint accepted for publication to "*International Journal of Wildland Fire***"** https://doi.org/10.1071/WF21076

Characterisation of thunderstorms that caused lightning-ignited wildfires

Anna Soler[A], *Nicolau Pineda*[A,B,D], *Helen San Segundo*[A], *Joan Bech*[C] *and Joan Montanya*`[B]

[A]Meteorological Service of Catalonia, Carrer Berl´ın 38-46, 08029, Barcelona, Spain. [B]Lightning Research Group, Technical University of Catalonia, TR1, Carrer Colom 1, Terrassa, 08222, Spain. [C]Department of Applied Physics – Meteorology, University of Barcelona, Barcelona 08028, Spain. [D]Corresponding author. Email: nicolau.pineda@gencat.cat

Abstract. This work studies the characteristics of thunderstorms that cause lightning-caused wildfires in Catalonia, north-east Iberian Peninsula, using lightning and weather radar data. Although thunderstorms produce ,57 000 cloud-to-ground (CG) flashes yearly in Catalonia, only 1 in 1000 end up as a flaming wildfire. Characterisation of thunderstorms that ignite wildland fires can help fire weather forecasters identify regions of increased ignition potential. Lightning data and radar products like maximum reflectivity, echo tops heights and equivalent liquid content were obtained over a 7-year period. Characteristics of thunderstorms that ignite wildfires are examined including storm motion, duration, morphology and intensity. It was found that most probable ignition candidates are lightning associated with cellular thunderstorms and non-linear systems. Radar reflectivity values for lightning that ignites wildfires were found to be below average, these morphological types favouring the occurrence of lightning outside regions of high reflectivity, where precipitation reaching the ground is low or non-existent. Thunderstorms that ignite wildfires are typically of low intensity, with a CG flash rate below average. Most ignitions occur during the maturity phase when the CG flash rate is the highest. A better scientific understanding of the thunderstorms that cause lightning wildfires will help improve early firefighting response.

Keywords: lightning, lightning-ignited wildfire, lightning location system, weather radar, thunderstorm tracking, Catalonia.

Received 31 May 2021, accepted 28 September 2021, published online 16 November 2021

Introduction

Wildfires cause substantial socio-economic losses and impact natural biodiversity in Mediterranean areas. In the southern European Union (EU) countries (Portugal, Spain, France, Italy and Greece), ,47 650 fires every year burn 448 400 ha on average (1980–2018), and a small number of large fires (,5%) account for the bulk of burned area (San-Miguel-Ayanz *et al.* 2019). Causality records from the European Fire Database (Camia *et al.* 2010) show that wildfires in the Mediterranean countries are mostly related to human activity (56% deliberate action, 33% negligence, 6% accidental). Contrarily to boreal forests, where lightning ignitions predominate (e.g. Stocks *et al.* 2002; McGuiney *et al.* 2005; Veraverbeke *et al.* 2017), and to the European Alps, were lightning fires account for up to a third of forest fires and burned area during the summer months (Cesti *et al.* 2005; Conedera *et al.* 2006; Mu¨ller *et al.* 2013; Moris *et al.* 2020), lightning is a minor cause of forest fires in the southern EU countries (5–10%). Therefore, little attention has been paid to lightning-ignited wildfires (hereafter, LIWs) in the area. Nonetheless, LIWs must be considered a major disruptive agent in Mediterranean-climate regions as they can trigger large fires (San-Miguel-Ayanz *et al.* 2013). Although most of the LIWs burn less than 1 ha, some of the largest fires recorded in Spain were caused by lightning (e.g. the 1994 Villarluengo and Millares wildfires with 75 000 burned ha, Fernandes *et al.* 2021). In Mediterranean ecosystems, fires usually burn under extreme meteorological conditions (e.g. Oliveras *et al.* 2009). Extended dry spells are conductive to extended periods of low fuel moisture (e.g. Jain *et al.* 2017); the drying of soils and vegetation allows increased opportunities for fire ignitions and can generate more severe fires (Westerling *et al.* 2006). Under these conditions, intense storm systems can cause multiple, fairly simultaneous LIWs (e.g. Keeley and Syphard 2021). In addition, since lightning ignitions can occur anywhere, ignitions in complex topography can be challenging, leading to complex LIW episodes that may overwhelm fire brigades, resulting in longer response times and more difficult firefighting campaigns (Costafreda-Aumedes *et al.* 2016). A significant example was the California 2020 wildfire season, where lightning complex fires, like the Sonoma–Lake Napa Unit (LNU) and the Santa Clara Unit (SCU) burned 147 000 and 160 000 ha respectively, causing six fatalities and significant economic and

environmental impacts (Department of Forestry and Fire Protection of California, https://fire.ca.gov/).

Wildfires are driven by the availability of fuel, oxygen and heat (the so-called fire triangle, Pyne *et al.* 1996). Ignition sources can be natural or anthropogenic. Among natural causes, lightning is the most important source worldwide (Komarek 1964; Pyne *et al.* 1996). It is generally accepted in scientific literature that lightning with long continuing current (LCC, a continuing current component that lasts longer than ,40 ms; Brook *et al.* 1962; Kitagawa *et al.* 1962) heats the fuel for longer and consequently has a higher capacity to ignite a fire (Fuquay *et al.* 1967; Fuquay 1980; Latham and Williams 2001). High-speed video observations (e.g. Ballarotti *et al.* 2005; Campos *et al.* 2007; Saba *et al.* 2006, 2010; Montanya` *et al.* 2012; Pineda *et al.* 2014) have shown that, although LCC is not present in all lightning flashes, it is present with both polarities. However, LLC is more common in positive cloud-to-ground (þCG) flashes (65–75%) than in negative cloud-to-ground (–CG) flashes (20–60%). As þCG have a major probability of ignition, past research focused on this type of lightning (Fuquay 1982; Rust *et al.* 1985; Latham and Schleiter 1989). However, since –CG climatologically outnumber CG (80–90% *v.* 10–20%), in the end, the majority of LIW are ignited by negative flashes (e.g. Pineda *et al.* 2014; Schultz *et al.* 2019; Moris *et al.* 2020).

Most lightning flashes occur within the rain shaft of a thunderstorm, under the thunderstorm convective core. Many studies have established positive correlations between lightning production and high radar reflectivity (35–40 decibels of reflectivity, dBZ) volume above the –108C isotherm height (e.g. Dye *et al.* 1989; Williams *et al.* 1989; MacGorman *et al.* 1999; Liu *et al.* 2012; Salvador *et al.* 2020). This relationship can be explained by the dominant charging mechanism in most thunderstorms, a non-inductive process (Takahashi 1978; MacGorman *et al.* 2008) that involves rebounding collisions within the mixed-phase environment, wherein hydrometeors of multiple phases coexist: graupel pellets, ice crystals and supercooled liquid water (Williams *et al.* 1991; Deierling *et al.* 2005). In a classical, convective-scale thunderstorm, where the ascent is provided by conditional instability and the release of convective available potential energy, the electrical structure consists of a vertical tripole, with a dominant middle negative charge region and positive charge regions above and below (Krehbiel 1986; Williams 1989; Stolzenburg and Marshall 2008). This typical layer configuration favours the production of CG lightning (Tessendorf *et al.* 2007; Stolzenburg and Marshall 2008; Salvador *et al.* 2021). However, the majority of lightning-caused ignitions under convective cores are extinguished by concurrent heavy rainfall. In contrast, a small fraction of CG flashes strike outside the main core with very little or no nearby concurrent rainfall (e.g. Hall 2008; Dowdy and Mills 2012; Vant-Hull *et al.* 2018; Mu¨ller and Vacik 2017; Pineda and Rigo 2017). Rorig and Ferguson (1999) defined those strikes as 'dry lightning', as they occur with rainfall less than 2.54 mm (0.1 inches). In the present study, we use a threshold of less than 2 mm precipitation (Pineda and Rigo 2017). Ignitions caused by dry lightning are more likely to produce flaming wildfire because precipitation reaching the ground is weak or non-existent. Despite the probability of ignitions having been related to lightning density (e.g. Latham and Schleiter 1989), the survival phase is highly dependent on fuel moisture, and that is why the concept of dry lightning is of importance (Dowdy and Mills 2012; Nauslar *et al.* 2013). Therefore, the probability of LIW occurrence depends not on the probability of ignitions, but on the fraction that eventually survives the thunderstorm.

Fuel moisture content is increased by groundwater availability, atmospheric humidity and especially precipitation (e.g. Flannigan and Wotton 1991; Evett *et al.* 2008; Morin *et al.* 2015). The relative timing between the lightning strike and precipitation, which is critical to whether lightning ignitions survive and turn into flaming combustion, is a key issue for understanding lightning-caused ignitions (Hall 2007). Past research has dealt with the relationship between lightning-ignited wildfires and precipitation (e.g. Pineda and Rigo 2017). There has also been a significant amount of research concerning radar reflectivity related to thunderstorms and lightning (e.g. Williams *et al.* 1989; Carey and Rutledge 1996; MacGorman *et al.* 1999; Rigo *et al.* 2010, Salvador *et al.* 2020) but there has been little research linking radar-derived thunderstorm patterns with the locations of lightning-ignited wildfires (Hall 2008).

The acquisition of quantitative data on lightning-ignited wildfires is challenging yet critical to improve our current knowledge on natural wildfire processes. This lack of data limits the understanding of this wildfire–atmosphere interaction and hampers the ability to model and predict its occurrence. There has been limited research analysing naturally ignited wildfires in relation to storm structure and lifecycle. In this regard, the present study aims to improve the characterisation of wildfire-producing storms. By adding weather radar data to the systematic analysis of LIWs, a better understanding of the characteristics of thunderstorms that trigger LIWs can be acquired. In doing so, the present study aims to shed new light on some observations reported in past research. Namely, Kera¨nen (1929), Kitterman (1980) and Granstro¨m (1993) suggested that isolated afternoon storms are more likely to generate a fire than storms associated with a front crossing. According to Larjavaara (2005), the probability of ignition is higher in low-intensity storms, because although there is less lightning, these have little associated precipitation and therefore a possible ignition is more likely to end in a fire. Rorig and Ferguson (2002) and Larjavaara (2005) suggest that in areas across which a storm has moved rapidly, there is a lower accumulation of rain that leads to an increase in the probability of ignition of a fire. According to Hall (2008), the discharges most likely to cause fires occur on the margins of storms, where precipitation reaching the ground is low or even non-existent. Consequently, the fact that storms with smaller areas have relatively a larger ratio of perimeter to area than storms over large areas makes the probability of ignition higher on days when there are many small storms than on days with fewer but more extensive storms (Flannigan and Wotton 1991). While this series of works gives an idea of which kind of storms generate LIWs, a systematic study is needed to objectively characterise wildfire-producing storms. Although the datasets and methods of the current study partially overlap with those in prior studies (Pineda *et al.* 2014; Pineda and Rigo 2017), the current study extends the science of these earlier works to the study of LIW parent thunderstorms.

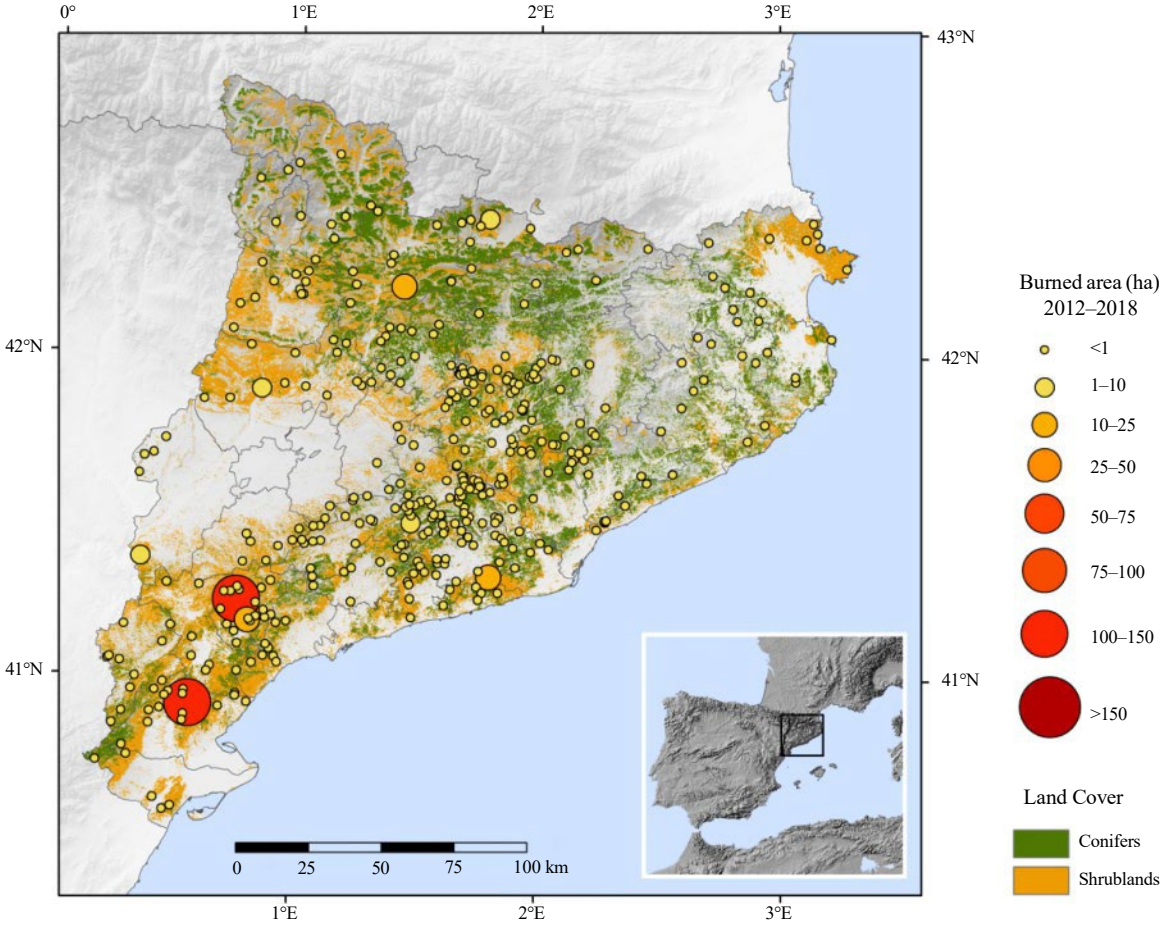

Fig. 1. Geographical distribution of lightning-ignited wildfires for the 2012–2018 period in Catalonia (NE Iberian Peninsula). The size of the circle is proportional to the burned area. Wildfire data source: Forest Protection Agency, Autonomous Government of Catalonia. Land cover map data source: land cover map of Catalonia (https://www.creaf.cat/ca/land-cover-map-catalonia).

Data

The study area was Catalonia, a region of ,32 000 km^2 in the north-east of the Iberian Peninsula, in the north-west of the Mediterranean basin (Fig. 1). Two main geographical features delimit the region: the Pyrenees mountain range on the northern border, and the Mediterranean Sea along the SW–NE coastline. Regarding forest fires caused by lightning, another relevant orographic feature is the pre-littoral mountain range (1000–1700 m above sea level (asl)) that runs parallel to the Mediterranean coastline and encompasses a significant number of LIWs (Fig. 1). Catalonia's Mediterranean climate, with hot and dry summers, prolonged drought periods and strong winds (Mart´ın-Vide *et al.* 2010), plays a significant role in the Mediterranean fire regime (Ganteaume *et al.* 2013). Catalonia is extensively covered with forests and shrublands: ,60% of the country is forest land according to the Ecological Forest Inventory of Catalonia (IEFC, Gracia *et al.* 2004). Dominant tree species where most of the LIW take place (Fig. 1) are conifers, like *Pinus halepensis*, *Pinus nigra* and *Pinus sylvestris*. Additionally, these conifer stands have abundant highly flammable species in the understorey like *Erica* sp., *Genistella tridentata* and *Calluna vulgaris*, among others, which contribute to fire propagation after ignition (Rodr´ıguez-Pe´rez *et al.* 2020). Moreover, the IEFC reported a significant increase of 3.2% in forest land cover between1966 and 2001, mainly related to rural exodus. Indeed, forest fires are an increasing natural hazard (e.g. Llasat-Botija *et al.* 2007), owing to land use changes that have increased the wildland–urban interface and promoted homogeneous forest landscapes and forest fuel accumulation (Badia *et al.* 2002; Gonza´lez and Pukkala 2007; Alcasena *et al.* 2019).

Since 1986, the Forest Protection Agency of the autonomous government of Catalonia (Servei Prevencio´ Incendis Forestals, SPIF) has managed the governmental wildfire database. Records include information on the cause of ignition, and the date, time and coordinates of the point of ignition. Based on the available data, there are 640 wildfires a year, which burn 7700 forested ha per year, on average. Large fires (.100 ha) account for more than 88% of the burned area. Wildfires caused by lightning only represent 10.4% of the total number of wildfires and 2% of the burned area. There have been 2250 wildfires due to lightning since 1986, thus an average of 66 LIWs per year. Most of them occur during summer, the months from June to September encompassing 90% of the LIWs.

During the period of the present study (2012–2018), lightning caused 393 LIWs, with an average of 56 wildfires per year and 200 burned ha per year. The burned area rarely exceeded 1 ha per LIW (Fig. 1). These 7 years were selected based on the availability of radar data; however, the yearly average of LIWs is representative of the longer SPIF record.

Lightning data used in the current study were provided by the Servei Meteorolo`gic de Catalunya (SMC) lightning location system (hereafter SMC-LLS). This LLS is composed of four total lightning detectors (Vaisala LS-8000). Individually detected CG strokes are grouped into CG flashes using an algorithm based on time and distance criteria (Cummins *et al.* 1998; San Segundo *et al.* 2020). The performance of the SMC-LLS is periodically evaluated (see Pineda and Montanya` 2009 for details on the evaluation methods). These periodical evaluations indicate a CG flash detection efficiency (DE) of ,85–90% for the SMC-LLS.

Weather radar was used to determine the characteristics of the thunderstorms that produce LIW in the study region. The SMC operates a weather radar network composed of four C-band (5.600 to 5.650 MHz) Doppler radars. Polar volumes are acquired every 6 min, in a 16-elevation scan scheme. Radar volumes include 16 plan position indicator (PPI) scans every 6 min, the scan range being 130 km. Time-synchronised volumetric data from individual radars are combined into a single three-dimensional volume, which is used to generate composite products like the Constant Altitude Plan Position Indicator (CAPPI). Radar composite products allow a substantially improvement in individual radar coverage, which otherwise is limited by orographic beam blockage in several sectors (Bech *et al.* 2003; Trapero *et al.* 2009). Further details of the SMC radar network can be found in Bech *et al.* (2004) and Argem´ı *et al.* (2014).

Methods

Most probable candidate

The first step seeks to identify the fire starter for each of the LIWs that took place in Catalonia between 2012 and 2018. To this end, two independent datasets are combined: the SPIF wildfire and the SMC-LLS databases. The first step looks for all lightning occurring in the vicinity of the wildfire (10 km radius) within the previous 72 h. In a second step to select the most probable candidate (hereafter MPC) among the lightning flashes located close to each wildfire, we used the method described in Pineda *et al.* (2014), which, in turn, is an adaptation of the 'proximity index' proposed by Larjavaara *et al.* (2005) (Eqn 1). The proposed probability distributions as a function of time (*T*) and distance (*S*) are linear and assume that a stroke with $T = 0$ and $S = 0$ is certainly the fire starter:

$$A = \left(1 - \frac{T}{T_{max}}\right) \times \left(1 - \frac{S}{S_{max}}\right) \quad (1)$$

where T_{max} defines the longest considered holdover time (72 h) and S_{max} the maximum buffer radius around the ignition point (10 km). The MPC is therefore the lightning stroke with the highest *A* score. Once the MPCs are identified, the time span between the lightning occurrence and the wildfire start date (the holdover period) is determined for each LIW, subtracting the start time of the wildfire report from the time of the MPC. Holdover times greater than 3 days are rare in the study area (Pineda and Rigo 2017); thus, generally at least one candidate is to be found within the previous 72 h. In the case where no lightning candidates are found, the time period is extended to 10 days.

Characteristics of lightning

At present, LLSs locate lightning CG strokes with high efficiency and precision. However, ground-based LLSs rely on the strong peak current of the return strokes, but fail to detect weak current signals like those coming from the LCC component. Therefore, all lightning reported by the LLS has to be considered as a potential ignition candidate. Past research focused on the use of lightning attributes like multiplicity, polarity and peak current as a proxy for wildfire ignition, given the possible dependence of LCC on polarity and multiplicity (e.g. Latham and Schlieter 1989; Latham and Williams 2001; Durden *et al.* 2004). However, currently this approach seems ineffective as later studies have found that the multiplicity and peak current of igniting lightning candidates are not substantially different from those of the rest of lightning (e.g. Larjavaara *et al.* 2005; Hall and Brown 2006; Nieto *et al.* 2012; Pineda *et al.* 2014; Mu¨ller and Vacik 2017; Schultz *et al.* 2019). Nevertheless, lightning attributes from the MPC selection were compared with lightning climatology.

Thunderstorm selection

Once a lightning flash has been identified as the MPC for each LIW, the next step is to find the parent thunderstorm that produced the MPC. To this end, two independent datasets are combined: the SMC lightning database and the SMC storm tracking database (Rigo *et al.* 2010). Here, the MPC is associated with the closest storm cell object within the 6-min time span to which the lightning belongs. This association was manually supervised using the CAPPI product using geographic information system (GIS) techniques. Although it was a time-demanding task, it was considered necessary since the MPC can be in the stratiform region of the storm system, outside the convective core (storm cell object). Once the parent storm is identified and validated, lifetime characteristics of the LIW parent thunderstorm are retrieved from the SMC storm tracking database.

Storm morphology

Thunderstorm systems producing LIWs were also analysed in terms of storm morphology. The selected LIW parent thunderstorms (hereafter, LIW-PTs) were classified according to their dominant storm morphology, using the classification system developed by Parker and Johnson (2000) and Gallus *et al.* (2008) based on the analysis of weather radar reflectivity CAPPI sequences. As pointed out by Duda and Gallus (2010), classifying convective systems by visual inspection of radar data is somehow subjective, but the quantitative guidelines contained in the method should reduce subjectivity. Gallus *et al.* (2008) defined nine morphologies (Fig. 2). Three of them are of the cellular type: isolated cells (ICs); clusters of cells (CCs), and

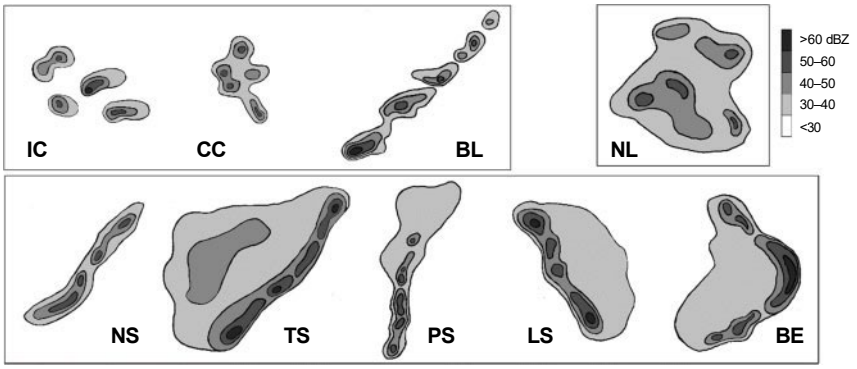

Fig. 2. Schematic drawings of the systems for each of the nine storm morphologies, grouped in three general morphological types. Cellular type: IC, isolated cells; CC, cluster of cells; BL, broken line of cells. Non-linear type: NL, non-linear convective system. Linear type: NS, squall line with no stratiform precipitation; TS, trailing stratiform precipitation; PS, parallel stratiform precipitation; LS, leading stratiform precipitation; BE, bow echo. Storm motion is left to right in all cases. Adapted from Gallus *et al.* (2008).

broken lines (BLs). Five morphologies are of linear type: squall line with no stratiform precipitation (NSs), trailing stratiform squall lines (TSs), parallel stratiform squall lines (PSs), leading stratiform squall lines (LSs), and bow echoes (BEs). Finally, one last type is defined as non-linear convective morphology (NL).

Storm tracking

Among other applications, SMC radar data feed an operational thunderstorm tracking system (see Rigo *et al.* 2008, 2010 and del Moral *et al.* 2020 for details). The SMC storm tracking algorithm is a local adaptation of the well-known SCIT algorithm (Storm Cell Identification and Tracking Algorithm; Johnson *et al.* 1998). A detected storm cell is tracked in successive radar images (6-min time span), allowing a time history of the cell displacement to be derived. The characteristics of these cell objects describe the storm structure and their attributes are computed from the volumetric radar data. Storm attributes include cell reflectivity (average and maximum), echo tops height (12 and35 dBZ), and Vertically Integrated Liquid (VIL). The EchoTops product refers to the maximum height of radar echoes with a reflectivity equal to or higher than a given reflectivity threshold. The EchoTops-12 product can be taken as an indicator of the altitude of the thunderstorm top boundary (e.g. Rosenfeld *et al.* 1993; Yuter and Houze 1995), whereas EchoTops-35 is a proxy for the maximum convective intensity of precipitation (e.g. Vincent *et al.* 2003; Yang and King 2010; Liu *et al.* 2012; Salvador *et al.* 2020). Further, the VIL content, obtained by vertical integration of radar reflectivity (Greene and Clark 1972), may be more representative of the amount of rainfall estimated to reach the ground compared with the maximum reflectivity. High values of VIL generally indicate a very dense column of water or ice present in the storm (Metzger and Nuss 2013) and have shown a statistically significant correlation with lightning intensity (Steiger *et al.* 2007).

Finally, the CG flash rate was calculated for thunderstorm cell objects in a 6-min time bin framework corresponding to the time span of the tracking algorithm. Three categories of intensity were considered (Rigo *et al.* 2010): weak (,2 CG flashes min^{-1}), moderate (2–10 CG flashes min^{-1}) and intense (. 10 CG flashes min^{-1}).

Results

Characteristics of lightning that ignites wildfires

Since LLS does not detect the LCC component, flash multiplicity, polarity and peak current of the return stroke were used as proxies for wildfire ignition likelihood. Table 1 presents a comparison between the MPCs and the whole population of lightning recorded over Catalonia for the period of study. Although there is 7% more þCG in the MPCs compared with the whole dataset, the MPC sample has almost 3/4 of –CG. As expected, peak currents were higher in positive than in negative MPCs. Regarding multiplicity, and in spite of displaying similar peak currents, –CG flashes that ignite wildfires had almost three CG strokes per flash, higher than the average (1.7). On the other hand, MPC þCG flashes had a lower average peak current and a higher multiplicity (1.9) compared with the average (1.3). All in all, from the above numbers, no substantial differences can be clearly established between MPCs and average population characteristics. The small differences found can be due to the huge difference in the number of samples, the figures for the small LIW sample not being statistically significant. In fact, the probability of a discharge causing a fire owing to the peak current, through Bayes' theorem, showed that probabilities were very low among all the range of peak currents.

Therefore, all kind of lightning can be at the origin of an LIW. Ignition is either started by negative and positive CG flashes, as well as by a wide range of first-stroke peak currents in both polarities. Despite the reported differences, from a practical point of view, no lightning can be discarded as the ignition source of an LIW by analysing its LLS-measured attributes.

Characteristics of the parent storms

First, the 371 storms resulting from the LIW–thunderstorm matching, through MPC identification, were analysed in terms of morphology, trajectory, speed, covered distance and duration. Second, the analysis focused on the time of occurrence of the

MPC in relation to the storm life cycle. The timing of the LIW was compared with the phase of the LIW-PT, as well as radar-derived parameters for the MPC like reflectivity (Z), EchoTops and VIL. An example illustrating centroid tracking is shown in Fig. 3. The radar-derived 24-h accumulation of the quantitative estimated precipitation (Trapero *et al.* 2009) is overlaid on the tracking centroids of the LIW parent cell for the 2 October 2016 LIW. This episode was first detected at 1130 UTC (Universal Time Coordinated) and had a duration of almost 2 h, travelling ,30 km. Derived tracking cell centroids (whose colour symbols represent time progress with darkening grey shading) show how the LIW-PT followed a rather straight path, the LIW occurring practically at the end of the lifecycle (1319 UTC). The flaming LIW was observed at 1355 UTC (shown as a red star). Underlying rainfall throughout the episode shows lower accumulations at the end of the episode, coinciding with the location of the lightning ignition (shown as a red diamond).

Table 1. Average statistics for all cloud-to-ground flashes recorded in Catalonia (SMC-LLS) in 2012–2018 and for most probable candidates (MPCs) of wildfire ignition

Flash polarities and peak currents refer to the first stroke of each flash. Multiplicity is the average number of strokes per CG flash. The percentage of single-stroke flashes is also reported

	All flashes	MPC
Sample	393 423	371
Polarity		
Negative (%)	85	77
Positive (%)	15	23
Multiplicity (strokes per CG flash)		
Negative (%)	1.7	2.9
Positive (%)	1.3	1.9
Single-stroke CG flashes		
Negative (%)	59	39
Positive (%)	77	43
Average (median) CG peak current		
Negative (kA)	–16.6 (–11.6)	–17.7 (–12.8)
Positive (kA)	þ33.4 (þ20.3)	þ23.6 (þ13.3)

All LIW-PTs were classified through visual inspection of radar CAPPI sequences, according to the storm morphology of Gallus *et al.* (2008). It is worth noting the difficulty of the classification process, given that the convective system may exhibit changing morphologies throughout its lifetime. Following the recommendations of Duda and Gallus (2010), the dominant morphology was considered to represent the whole episode. The contribution of each morphology to the total sample of LIW-PTs is shown in Fig. 4*a*. The three most common systems (NL, CC and IC) account for 3/4 of the sample. The largest single contributor is the NL category, constituting almost half of the sample. In part, this may be due to the fact that the cases that are difficult to classify generally end up in this category. Regarding broad morphological types (cellular, linear and non-linear), non-linear systems account for the greatest portion of all LIW-PTs in the dataset (47%), followed by cellular systems (38%) and linear systems (15%).

As no previous reference for this storm morphology classification existed in the study region, the LIW frequency distribution was compared with the classification of Duda and Gallus

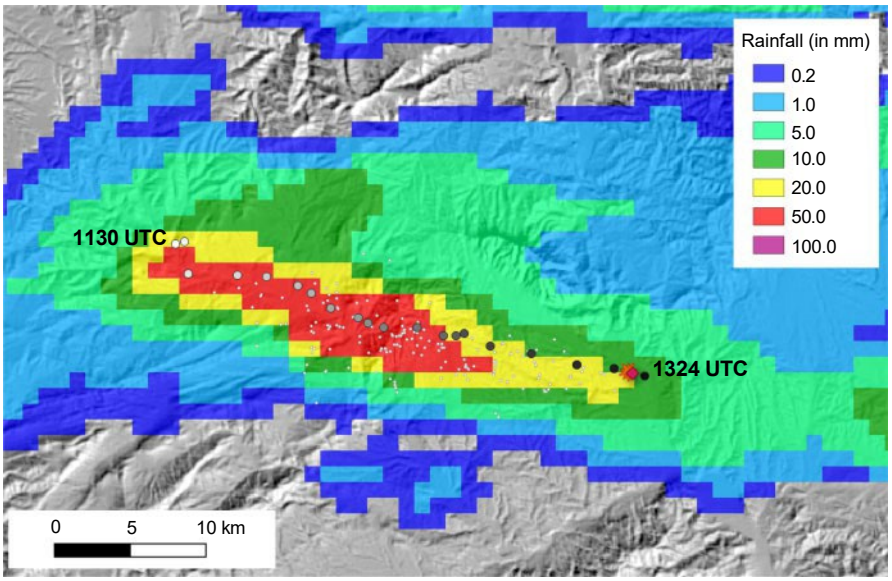

Fig. 3. Example of the lifecycle of a lightning-ignited wildfire parent thunderstorm, which took place on 2 October 2016. The storm evolution is represented through the 6-min radar-derived centroids produced by the tracking algorithm. The storm evolved from west to east, starting at 1130 UTC and travelling ,30 km in 2 h approximately. The most probable candidate for the ignition (red diamond) occurred at the very end of the storm (1319 UTC); the lightning-ignited wildfire was reported at 1355 UTC (shown as a red star). Storm evolution is overlayed onto the 24 h radar-derived rainfall accumulation (in mm) and the shadowed digital elevation model (grey levels).

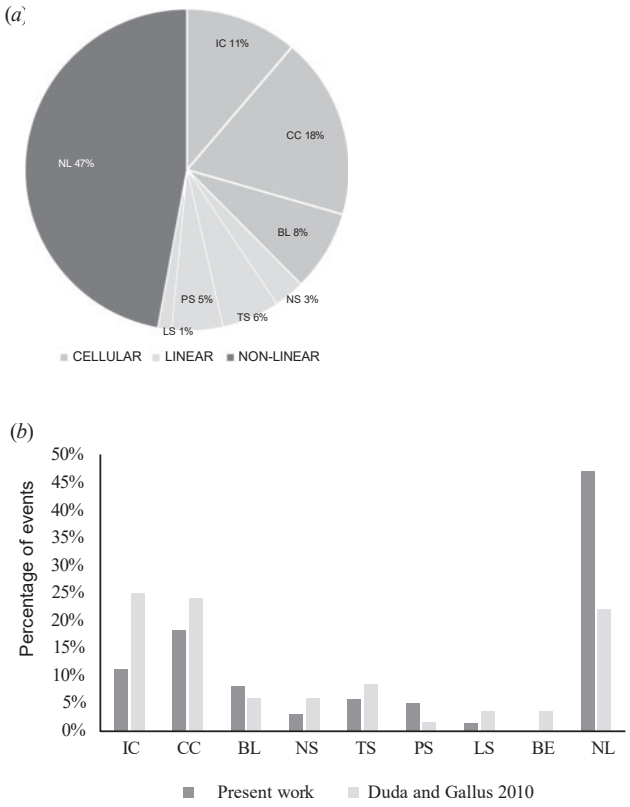

Fig. 4. (*a*) Percentage contribution of each morphology to the total number of LIW. Shading corresponds to general morphological type: linear (light grey), cellular (medium grey) and non-linear (dark grey). Numbers indicate the percentage of events that occurred for each morphology. (*b*) Percentage of systems from each morphology, comparing the present work (dark grey) with Duda and Gallus (2010) (light grey).

(2010) for the Midwestern United States and Central Great Plains (Fig. 4*b*). Rankings of the three topmost-productive systems are the same in both datasets (NL, CC and IC), although there are substantial disparities in the percentages. It is worth pointing out that LIW episodes in which the SMC tracking system failed to detect or track the thunderstorm system resulted in NL systems when manually classified through the CAPPI sequences. Yet this may be a significant result of the morphology analysis: the higher percentage of NL systems suggests that LIW-PTs tend to be non-organised systems (difficult to track) dominated by cellular morphologies, and surrounded by stratiform areas bearing a larger number of CG strokes under moderate reflectivity regions (less ground-reaching precipitation at the ignition location), the related ignitions having a higher probability of survival and arrival.

Storm tracks

Time and location coordinates of LIW-PT starting and ending spots are derived from the SMC thunderstorm tracking algorithm (Fig. 5). The first point on a track represents the time and location of the first storm centroid, which in general is not the storm initiation spot. Since the starting point is irrelevant for the present study, no backward extrapolation is needed. However, in terms of duration, one should keep in mind that a time interval of approximately 10–15 min should be added both before and after the start and end timestamps from the tracking system. For the purposes of characterising the LIW-PT distribution of thunderstorm initiation, including or excluding this extra time and consequent covered distance will not significantly impact the results.

Visual analysis of the set of trajectories displayed in Fig. 5 reveals some of the local thunderstorm patterns. For example, storms initiated in the Iberian System mountain range (not shown, SW of the map) typically reach Catalonia from the SW and have a SW-to-NE bearing (e.g. Rigo *et al.* 2010). These SW-to-NE tracks generally present linear trajectories, associated with long-lived thunderstorms that last more than 1 h (del Moral *et al.* 2018). Thunderstorms in the Pyrenees (northern part) are clearly constrained by the local orography, as they usually follow valleys at a lower speed (closer centroids), compared with the rest. The messy central part of the map has a less clear pattern. Once all those SW–NE are removed (not shown), another local pattern can be seen: inland convection that travels NW to SE to finally reach the coastline. All in all, LIW-PT trajectories are not different from climatological ones.

The frequency distribution of the distances travelled by the LIW-PTs is plotted in Fig. 6*a*. As observed, 80% of the LIW-PTs covered distances between 10 and 80 km (median 37 km). To cover such distances, they needed 72 min on average, half of them lasting less than 66 min (Fig. 6*b*). Only 15% lasted more than 2 h. Average velocity was 10.5 m s^{-1}, and 80% of the LIW-PTs had velocities in the range of 4–17 m s^{-1} (Fig. 6*c*). Fig. 6*d* presents the LIW time of occurrence relative to the phase of the storm. Note that LIW timings along the LIW-PT lifecycle are normalised by the maximum duration of the LIW-PT. By doing so, occurrence can be analysed in relative terms. Fig. 6*d* shows that, although LIWs are slightly more probable in the second half of the storm, they can occur at any stage. Whereas thunderstorm cells in the maturity phase tend to present the bulk of CG flashes closely related to the high reflectivity cores, as the storm begins to decay, precipitation becomes more scattered spatially, and so does the distribution of CG strokes, hence decreasing the likelihood of spatial coincidence (e.g. Brown *et al.* 2002; Hall 2008). Mazur *et al.* (1986) observed that, during dissipation, lightning activity tends to spread outside the convective core.

Rigo *et al.* (2010) described the thunderstorm life cycle for ordinary thunderstorms in the present area of study. The dissipation phase, which covers approximately the last 20% timespan of the storm, only accounts for 10% of the CG lightning. Applying an analogy to the current case studies, the last bin of the normalised duration constituting the dissipation stage (Fig. 6*d*) would contain 10% of the lightning activity of the whole lifecycle, while encompassing more than 20% of LIW cases. Therefore, the probability of LIW per CG flash is doubled during this phase.

Radar characteristics

Keeping in mind that most CG flashes occurs within the rain shaft of a thunderstorm (e.g. Che`ze and Sauvageot 1997; Petersen and Rutledge 1998; Molinie *et al.* 1999; Soula and

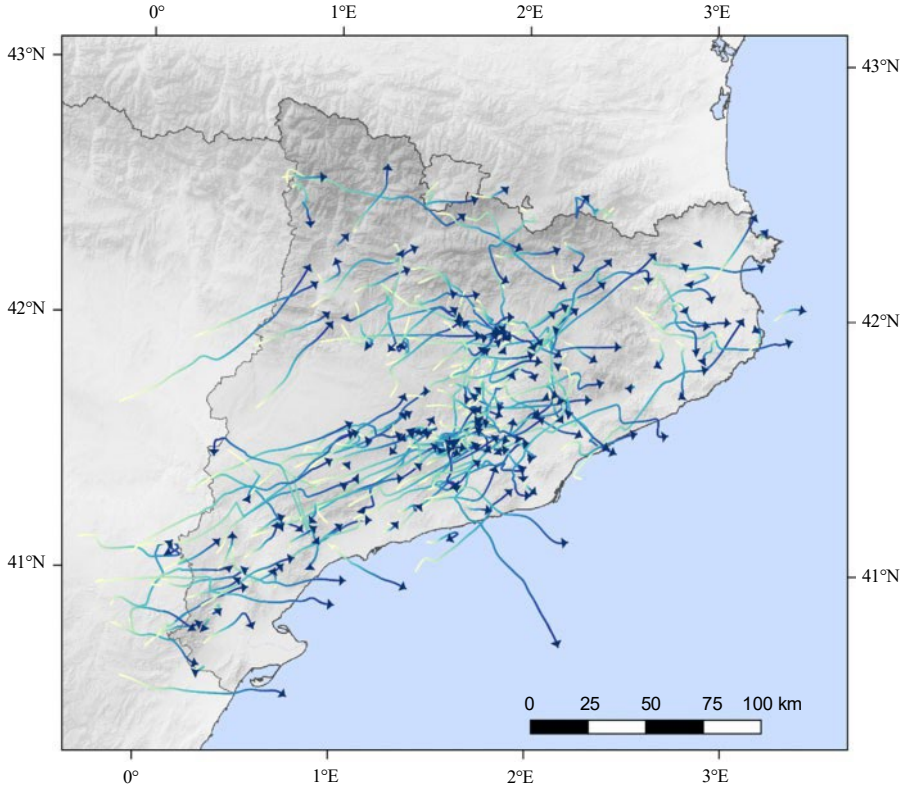

Fig. 5. Path of the LIW-PTs during the analysed period (2012–2018). The storm evolution, derived from the tracking algorithm, is represented through the 6-min radar-derived centroids. Colour ramp (blue – green – yellow) show storm evolution and duration. The base layer corresponds to the shadowed digital elevation model (grey levels).

Chauzy 2001; Pineda *et al.* 2007; Liu *et al.* 2012) and that only a small fraction strike outside the main core, the reflectivity associated with the MPCs was studied in detail. To do so, all lightning coordinates were analysed to resolve the maximum associated reflectivity. Results are presented in Fig. 7, in which the maximum reflectivity distribution of the MPC sample is compared with that of the rest of lightning that took place during the LIW-PT. In general, MPCs were related to lower values of maximum reflectivity. As many as half of the MPCs were outside regions of high reflectivity (below 36 dBZ), whereas the median for all CG flashes is at 42 dBZ. MPCs above 48 dBZ only comprise 5%, compared with 17% of all CG strokes. This suggests an increased probability of dry lightning being associated with air mass thunderstorms as precipitation is more likely to be within areas of high reflectivity. These results, similar to Hall's (2008), suggest that ignitions that survive and turn into flaming wildfires typically occur near the perimeter of the rain shaft.

Another approach for analysing the relationship of the LIWs with their parent storms is through radar products like EchoTops and VIL. Regarding the EchoTops-35 product, Fig. 8 shows LIW-related production areas of the thunderstorm to be of lesser intensity, compared with the frequency distribution of associated reflectivity for the whole CG activity. Besides, VIL values at the ignition location (Fig. 9) are below 5 mm in more than 90% of the cases, and below 2 mm in 60% of the cases. Such VIL magnitudes are sufficiently low to suggest that the precipitation reaching the ground, if any, is minimal and that the majority of the LIW can be related to 'dry lightning'.

CG flash rate

The CG flash rate for the whole life cycle of the LIW-PTs had an average of 1.2 CG flash min^{-1}, therefore being of weak intensity most of the time, according to the categorisation of Rigo *et al.* (2010). A shown in Fig. 10, maximum flash rates per storm throughout the whole lifecycle were between 1.2 and 5.5 CG min^{-1} (interquartile distance in MAX boxplot) and very few 6-min time bins had strong intensity (.10 CG min^{-1}). On the other hand, the 6-min bins containing the MPCs had intensities slightly larger than the median (Fig. 10). Concerning the intensity of the lightning activity at the moment of the LIW ignition, in one third of the episodes the MPC occurred when the flash rate was at its maximum. In 64% of the cases, the flash rate was above the lifecycle average. At the other end, in 13% of the episodes the MPC occurred when the activity was very low (below 10% of the thunderstorm maximum), which tends to occur at the very beginning or the later end of the storm.

Discussion

Method uncertainties

As pointed out by Moris *et al.* (2020), there are no datasets that unambiguously relate igniting lightning to the corresponding

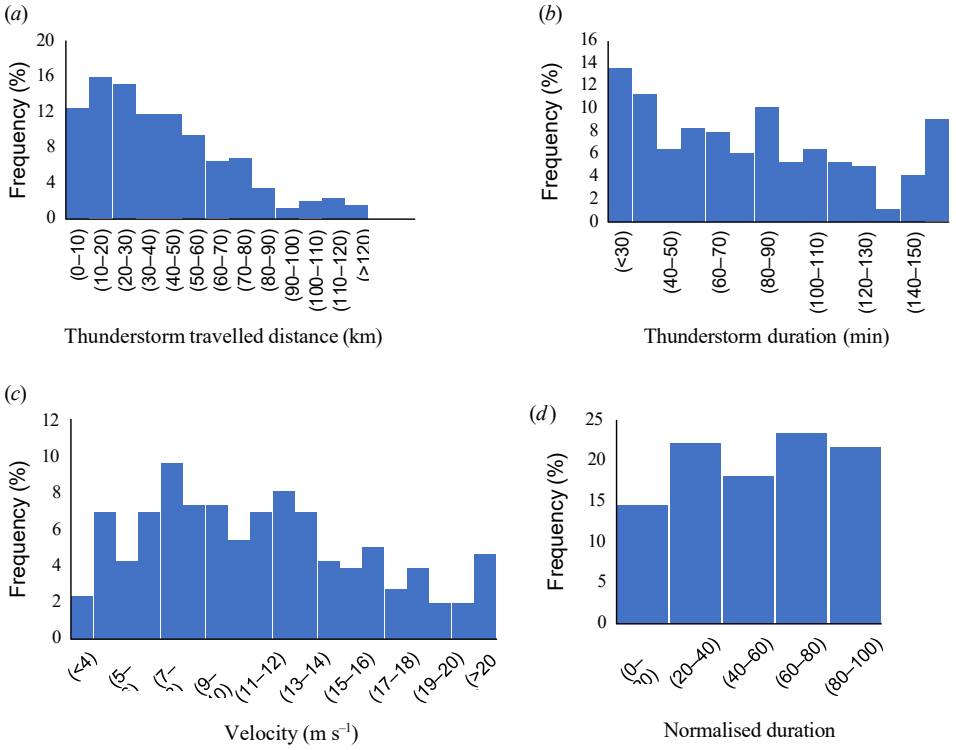

Fig. 6. Frequency distributions for (*a*) thunderstorm distance travelled (km); (*b*) thunderstorm duration (min); (*c*) thunderstorm velocity (m s^{-1}); and (*d*) LIW time of occurrence through the thunderstorm normalised duration (%).

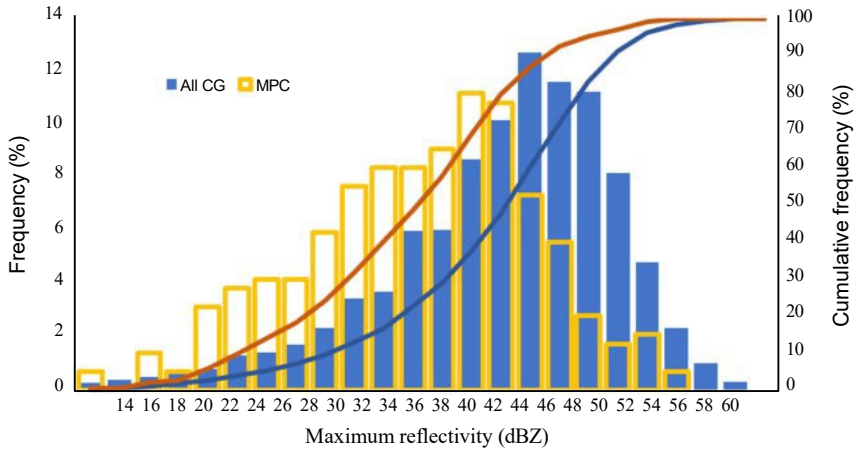

Fig. 7. Frequency plot and cumulative distribution of the maximum reflectivity (dBZ) associated with the most probable candidate (MPC) sample and the rest of cloud-to-ground lightning (All CG).

wildfires. From the original dataset of LIW cases considered, 22 had no lightning match-up (5.6% of the initial sample). Indeed, the process of pairing a lightning-initiated event with a lightning flash has some uncertainties.

Despite continuous improvements of LLSs and fire databases, the identification with absolute certainty of the individual CG lightning that triggered an ignition remains a challenge. On the one hand, the DE of LLSs, although having improved with time (e.g. Cummins and Murphy 2009; Nag *et al.* 2015; Schulz *et al.* 2016; Murphy *et al.* 2021), is still not 100%, since not all CG flashes are recorded. For instance, it is possible that the CG flash producing the LIW was not detected, especially if the peak amplitude was weak (Cummins and Murphy 2009; Nag *et al.* 2015). Regarding the SMC-LLS, validation field campaigns showed the DE for CG flashes to be of the order of 85–90% (Pineda and Montanya` 2009). The minimum detectable CG peak

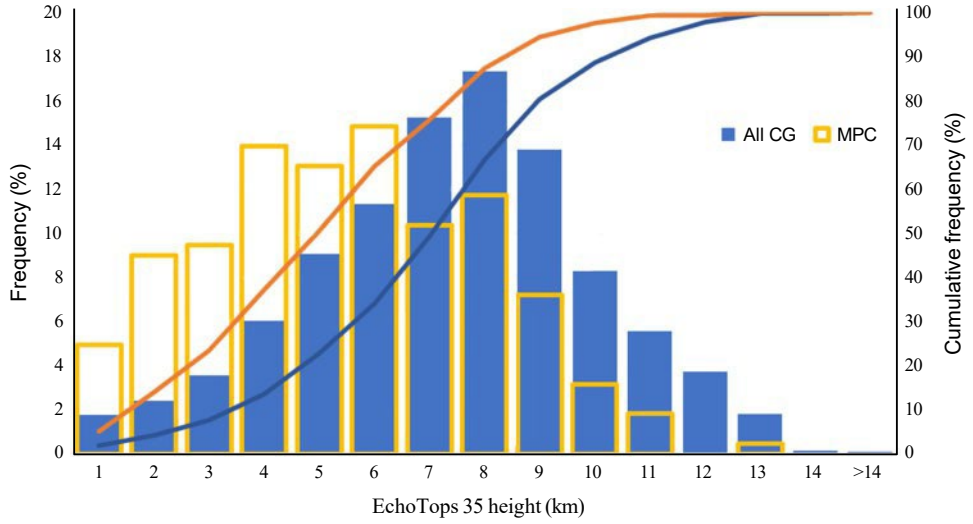

Fig. 8. Frequency plot and cumulative distribution of the EchoTops-35 associated with the most probable candidate (MPC) sample and the rest of cloud-to-ground lightning (All CG).

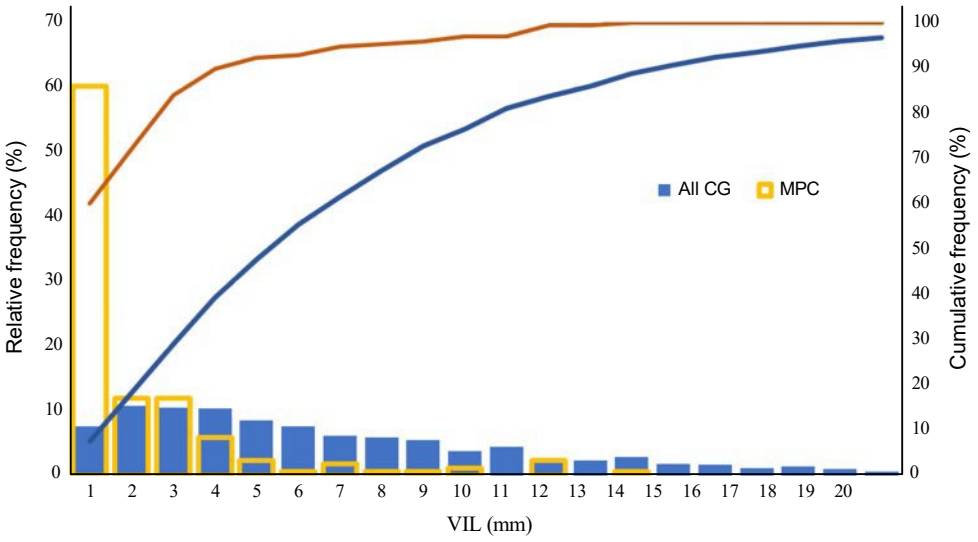

Fig. 9. Frequency plot and cumulative distribution of Vertical Integrated Liquid (VIL) content, the equivalent liquid amount of a given reflectivity column, associated with the most probable candidate (MPC) sample and the rest of cloud-to-ground lightning (All CG).

current ranged from 3 to 7 kA, as the system loses sensitivity when the distance to the centre of the network increases (March *et al.* 2014). Another constraint should be added regarding þCG, as small positive events (,10 kA) can actually be strong cloud pulses, and tend to be dismissed (Cummins *et al.* 2006). Still, a filter based on a peak current threshold will also remove small positives that are actually CG strokes (e.g. Cummins and Murphy 2009).

On the other hand, in terms of locational accuracy (LA), the geographical coordinates assigned to each CG stroke by the LLS correspond to the centre of a confidence ellipse (i.e. an area around the reported location within which there is a 50% probability that the CG stroke occurred; Cummins and Murphy 2009; Nag *et al.* 2015). Consequently, the actual coordinates of the strike at the ground are not known; thus, the assignment of a specific lightning strike to a specific ignition point is not unambiguous, especially in lightning-rich storms, where various candidates (and confidence ellipse areas) can be found in the vicinity of the ignition point. In the study area, the average value of the length of the major axis of the 50% confidence ellipse was of 0.90 km for 2012 and 2013 and slightly better (between 0.70 and 0.80 km) for the period 2014–2018.

Regarding the wildfire database, as the wildfire community is unsure exactly how long LIWs can smoulder, uncertainties include the possibility that the fire event was human-related but misclassified as lightning-related (MacNamara *et al.* 2020;

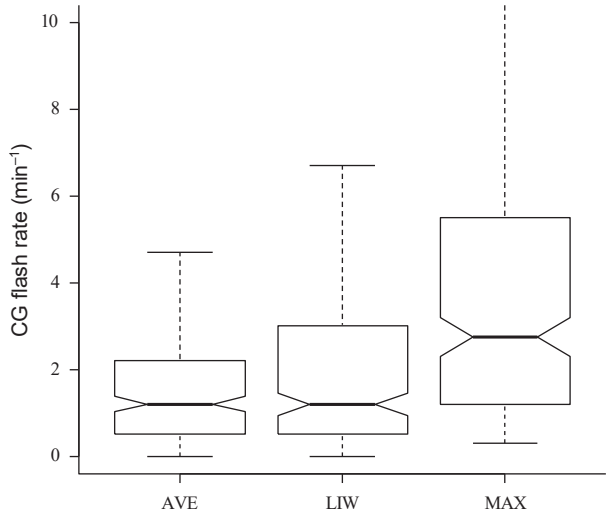

Fig. 10. Boxplot of CG flash rates: LIW-PT lifecycle average (AVE), on the 6-min bin containing the MPC that ignited the wildfire (LIW), and maximum attained by the LIW-PTs (MAX). Boxes represent the interquartile range between Q25 and Q75, with a solid line indicating the median value. Whiskers indicate the lower and upper limits of the 1.5 interquartile range; the notch represents the 95% confidence interval of the median.

Schultz *et al.* 2019). In relation to the present study, the SPIF wildfire database is regarded as a high-quality source for fire reports, since field investigation of the causes of a forest fire is carried out by trained personnel. The Corps of Rural Agents, among other tasks, assist firemen in forest fires, investigating the causes and effects of the fire, using standard methods based on physical evidence and public procedure. So, in the present case study, the missing match-ups can be mostly attributed to methodological constraints leading to undetected lightning.

Finally, the holdover time between ignition and arrival hampers the precise identification of the igniting lightning individual stroke, introducing uncertainty into the MPC assignation process (e.g. Dowdy and Mills 2012; Pineda and Rigo 2017; Schultz *et al.* 2019; Moris *et al.* 2020). The passage of different storms during previous hours (or even previous days) over the area of the wildfire can mask holdover fires that were ignited before the last storm crossing.

Lightning ignition efficiency

Bearing in mind that there are ,57 000 CG flashes per year in Catalonia, (SMC-LLS, average 2005–2020) and that the recorded LIWs are 56 per year (SPIF, average 2012–2018), the lightning ignition efficiency in Catalonia is ,1/1000. Although thunderstorms produce a lot more lightning ignitions (CG flashes with LCC are estimated to be between 25 and 65 per 100), only a few survive to eventually reach a flaming stage. Therefore, the ability to identify potential ignition candidates among the huge CG lightning annual population would be of great value to forest protection agencies.

Lightning attributes gathered by LLS about CG flashes like multiplicity, stroke polarity or peak current are not relevant in identifying the ignition likelihood of a particular CG flash. Comparison of the MPC sample with the whole dataset (Table 1) showed no significant differences, like in Pineda *et al.* (2014) who analysed a different period for the same study region. Other studies in the Alps (Mu¨ller and Vacik 2017; Moris *et al.* 2020) and in the USA (Schultz *et al.* 2019; MacNamara *et al.* 2020) also concluded that such attributes of fire starters are not substantially different from the rest of lightning. Still, there is higher proportion of þCG among MPCs, also reported by those studies, which is attributable to the fact that LCC is more frequent in þCG flashes than in negative ones (Anderson 2002; Saba *et al.* 2010; Pineda *et al.* 2014). Nonetheless, the MPC sample is dominated by _CG. As in Moris *et al.* (2020), these negative MPCs have a multiplicity above the average. Shindo and Uman (1989) showed that the multiplicity of negative flashes is positively correlated with the occurrence of LCC.

Given that CG lightning attributes are useless in identifying potential ignition candidates, other meteorological variables should be included in the decision-making process while preparing for days with multiple ignitions, routeing detection flight paths, and locating ignitions and potential holdover fires (Anderson 2002; Reid *et al.* 2010).

According to MacNamara *et al.* (2020), current United States Forest Service (USFS) metrics rely on the ground flash density (GFD, number of CG flashes per km^2) to set the probability of LIW occurrence: the larger the GFD, the greater probability of LIW to occur (Sopko *et al.* 2016). However, literature does not describe how GFD can be useful as a metric for wildfire prediction. In contrast, research suggests the greatest GFD to be spatially collocated with the highest rain rates (e.g. Che`ze and Sauvageot 1997; Petersen and Rutledge 1998; Molinie *et al.* 1999; Soula and Chauzy 2001; Pineda *et al.* 2007; Liu *et al.* 2012). Although the probability of ignitions is directly related to the GFD, a lightning ignition must overcome a complex process to eventually become a wildfire.

Forest fuel characteristics, especially moisture (which in turn is a function of the moisture in the environment), determine whether ignition will eventually survive or not (Flannigan and Wotton 1991; Meisner *et al.* 1993; Matthews 2014; Duff *et al.* 2017). In this regard, Pineda and Rigo (2017) explored, for the same study region, the relationship between lightning-ignited wildfires and precipitation. They showed that most LIW were related to dry lightning, as 25% of the MPCs had no associated precipitation at all, 40% had less than 2 mm of precipitation and 90% had less than 10 mm. Whereas daily rainfall accumulations used in Pineda and Rigo (2017) did not allow inferring the timing of the igniting lightning in relation to the different thunderstorm phases, the present results have shown that the probability of LIW per CG flash is doubled during the decaying phase of the storm (last 20% of the life-cycle).

Characteristics of LIW-PTs

Generally speaking, lightning starts in the leading edge of the developing storm (e.g. Mazur *et al.* 1986), moves close to high-reflectivity precipitation cores during maturity (e.g. Larjavaara 2005; Hall 2007), and spreads further into the radar cell in the decaying stages (e.g. Toracinta *et al.* 1996; Brown *et al.* 2002). With regard to lightning counts, Rigo *et al.* (2010) showed that, in the same study region, these concentrate in the maturity phase (80–90%), being scarce during development (5–10%) and dissipation (10–15%). Therefore, although Fig. 6*d* shows a rather

uniform distribution of the MPCs throughout the lifecycle, in relative terms there are more ignitions per lightning stroke at the developing and decaying stages. This could be useful information for predicting or anticipating natural wildfire ignitions.

Observations by Kera¨nen (1929), Kitterman (1980) and Granstro¨m (1993) suggested that isolated afternoon storms are more likely to generate a fire than storms associated with frontal systems. Similarly, Flannigan and Wotton (1991) found LIWs to be more common in thunderstorm systems composed of many small cells, compared with those with a few large cells. In this regard, Larjavaara (2005) and Hall (2008) suggested that smaller cells would produce scattered, lower-intensity precipitation, decreasing the likelihood that precipitation would either extinguish the fire or provide enough moisture to inhibit ignition. Further, Hall (2008) also pointed out that lightning most likely to cause fires occurs on the margins of storms, where precipitation reaching the ground is low or even non-existent. Consequently, the fact that storms with smaller areas have a proportionally larger perimeter than storms over large areas makes the probability of ignition higher on days when there are many small storms than on days with fewer but more extensive storms (Flannigan and Wotton 1991). The results of the present study have shown radar reflectivity values associated with MPCs to be below average, located outside regions of high reflectivity (below 36 dBZ), and mostly in non-linear (47%) and cellular systems (38%), morphological types that favour the occurrence of lightning on the margins of the thunderstorms' cores.

Thunderstorm distance travelled was estimated through storm track centroids. Most storms (60%) travelled between 10 and 45 km and few exceeded 100 km. This result seems to contradict Larjavaara (2005) who suggested that CG strikes from storms travelling further than 10 km are less likely to cause an ignition. It also differs from the results of Hall (2008), which indicated that two thirds of fire-causing thunderstorms travelled further than 50 km. However, geographical aspects may hamper this comparison. Orography is a leading mechanism in the spatial distribution of rainfall (e.g. Sotillo *et al.* 2003; Llasat *et al.* 2021) and also plays an important role in the development and evolution of thunderstorms in the study region (e.g. del Moral *et al.* 2020). In terms of duration, most of the LIW-PTs (96%) lasted less than 3 h, the median being 66 min. Keeping in mind geographical constraints, such duration results may be only comparable with those in Rigo *et al.* (2010), since the study region is the same. Rigo *et al.* (2010) found longer durations, which may indicate the LIW-PTs to be relatively shorter when related to the local climatology. In this regard, it is interesting to point out that Rigo *et al.* (2010) linked the duration of thunderstorms with the CG flash rate: the longer the duration, the higher the flash rate. This is reflected in the low flash rate of the LIW-PTs, with an average of 1.2 CG flash min^{-1}, therefore displaying a weak intensity most of the time (according to the categories in Rigo *et al.* 2010). Larjavaara (2005) suggested that the probability of ignition is below average in storms lasting more than 40 min, which would correspond to the isolated afternoon storms suggested in past research (e.g. Kera¨nen 1929; Kitterman 1980; Granstro¨m 1993). In our study, storm durations below 42 min represent one quarter of the sample approximately.

Analysis of the phase of the storm during which the MPC occurred reveals that, although ignitions may occur at any moment of the lifecycle, the probability of LIW per CG flash is higher during dissipation (last 20%) (Fig. 6*d*). This result does not match those of Hall (2008), who reported 93% of ignitions to occur in the first third of the storm lifecycle. Still, both results have in common that the probability of ignition is higher when both the rainfall and the flash rate are lowest, either in the developing phase or during dissipation. On the other hand, results also indicate that in one third of the episodes, the MPC occurred when the flash rate was at its maximum. Larjavaara (2005) suggested that the probability of ignition is lower during the maturity phase because that is when more precipitation is present and, despite more discharges, rain does not allow them to reach ignition point. In the present study, the MPCs occurred when activity was below 10% of the thunderstorm maximum only in 13% of the episodes, either at the very beginning or the end of the storm. In fact, the majority of MPCs occurred when the flash rate was above the lifecycle average; therefore, the lower precipitation associated with the MPCs is related to other factors, like the outer regions of the thunderstorm systems.

Besides a high rain intensity, heavy precipitation is also determined by the duration of rainfall: slow movement of the storm favours a longer duration of high rain intensities (e.g. Doswell 2001). In this regard, Rorig and Ferguson (2002) and Larjavaara (2005) suggested that the probability of ignition survival may increase in rapid storms. However, results displayed in Fig. 6*c* showed a wide range of storm speeds; thus, the storm speed does not seem to characterise LIW-PTs in the study region. The average speed of the analysed LIW-PTs was ,10 m s^{-1}, higher than that estimated by Hall (2008) for Arizona and New Mexico in the US (average 6.4 m s^{-1}). However, the different orography of these two regions may hamper a direct comparison.

Fire management implications

A better scientific understanding of the thunderstorms that cause lightning wildfires will help improve early firefighting responses. Models used for the prepositioning and deployment of firefighting brigades on the first dispatch can benefit from the results of this work. In fact, in southern European countries, the few fires that escape initial attack account for most of the burned area (Rodrigues *et al.* 2019). Simultaneous active fires, sometimes with a lightning origin, may hinder the chance of success in this initial attack (Costafreda-Aumedes *et al.* 2016; Rodrigues *et al.* 2019).

The suppression model remains the universal response to wildfire occurrence, the goal being to deploy all resources available to extinguish wildfires as quickly as possible (Pezzatti *et al.* 2013; Duff and Tolhurst 2015; Tedim *et al.* 2020). Over the past decades, these 'zero-tolerance' firefighting policies applied in central and southern EU countries have resulted in fuel accumulation, increasing the probability of potentially large and severe wildfires (namely the extinction paradox) (Minnich 1983; Castellnou and Miralles 2010; Brotons *et al.* 2013). Moreover, the strategy of reducing losses only by fire suppression has proved to be largely ineffective during extreme fire weather conditions (e.g. Alcasena *et al.* 2019). Based on the need to undertake a shift from fire suppression to fire management (e.g. Plana 2004), prescribed burning has been reintroduced to reduce fuel loads and diminish the risk of

high-intensity fires (e.g. Castellnou *et al.* 2010; Moritz *et al.* 2014). In this context, the role that lightning plays in the maintenance and evolution of forest ecosystems should be reviewed. Actually, LIW has always been part of Mediterranean ecosystems, as Mediterranean species are adapted to natural fire regimes with high recurrence and low intensity (Terradas 1996). Therefore, LIWs should be considered part of the new approach based on tolerating fire regimes with low-intensity fires. In fact, LIWs have already been allowed to burn under prescribed conditions in some national parks of the USA (van Wagtendonk *et al.* 2007). While considering the inclusion of LIWs in a broader fire management strategy in fire-prone southern European regions, there is a need to improve our current knowledge on the natural wildfire processes in Mediterranean ecosystems. In this regard, the wildfire management strategy developed by Alcasena *et al.* (2019) for Catalonia already identifies suitable areas for natural fire re-introduction, where LIWs pose a minimal risk to property and could positively contribute to fire-adapted ecosystem conservation (Barnett *et al.* 2016; Riley *et al.* 2018).

Conclusions

Although thunderstorms produce ,57 000 CG flashes each year in Catalonia, only 1 in 1000 end up as a wildland fire. Therefore, the ability to identify potential ignition candidates among the huge lightning annual population would be of great value to fire weather forecasters. In this regard, lightning characteristics like polarity, peak current and multiplicity have proved to be of little value. Adding weather radar data to the systematic analysis of LIWs can help to gain a better understanding on the characteristics of the thunderstorms that ignite wildland fires. Relevant characteristics found in the present work are summarised in the following:

- Most probable ignition candidates are lightning associated with radar reflectivity values below the average, located outside regions of high reflectivity (below 36 dBZ), mostly in non-linear systems (47%) and cellular thunderstorms (38%). These morphological types favour the occurrence of lightning on convective core margins (cellular type) and on adjacent stratiform regions (non-linear type), where precipitation reaching the ground is low or even non-existent (dry lightning). Under such conditions, the related lightning ignitions will have a higher probability of survival and arrival.
- LIW-PT life span analysis shows no typical distance covered, duration or velocity, while these characteristics appear to be more influenced by local thunderstorm patterns, related to dominant flows and local orography. Still, LIW-PTs are typically of low intensity, the CG flash rate being below average. Most successful ignitions, those turning into flaming wildfires, occur during the maturity phase, when the flash rate is the highest. The probability of ignition is slightly higher during the second half of the life cycle, presumably because precipitation becomes more spatially scattered, and so does the distribution of lightning. In terms of relative frequency, ignitions per lightning strike are higher during the decaying phase, which encompasses 10% of lightning but 20% of the LIW.

Data availability

Remote sensing data from Servei Meteorolo`gic de Catalunya that support this study are available in ZENODO at doi:. 10.5281/zenodo.5570522 Data from the wildfire database were obtained from Servei Prevencio´ Incendis Forestals (SPIF) by permission. Data will be shared upon reasonable request to the corresponding author with permission from SPIF.

Conflicts of interest

The authors declare no conflicts of interest.

Author contributions

Anna Soler: data curation, formal analysis, writing of original draft. Nicolau Pineda: conceptualisation, methodology, supervision, writing of original draft. Helen San Segundo: data curation, visualisation. Joan Bech: supervision, writing – review and editing. Joan Montanya`: funding acquisition, project administration, writing – review and editing.

Declaration of funding

This research was partially funded by research Grants ESP2015–69909-C5–5-R and ESP2017-86263-C4-2-R funded by MCIN/AEI/ 10.13039/501100011033 and by 'ERDF A way of making Europe', by the European Union; and Grant PIDP2019-109269RB-C42 funded by MCIN/AEI/ 10.13039/501100011033.

Acknowledgements

We acknowledge J.A. Tere´s at SPIF for providing access to the wildfire database of the Forest Protection Agency of the Autonomous Government of Catalonia.

References

Alcasena FJ, Ager AA, Bailey JD, Pineda N, Vega-Garc´ıa C (2019) Towards a comprehensive wildfire management strategy for Mediterranean areas: Framework development and implementation in Catalonia, Spain. *Journal of Environmental Management* **231**, 303–320. doi:10.1016/J.JENVMAN.2018.10.027

Anderson KR (2002) A model to predict lightning-caused fire occurrences. *International Journal of Wildland Fire* **11**, 163–172. doi:10.1071/WF02001

Argem´ı O, Altube P, Rigo T, Ortiga X, Pineda N, Bech J (2014) Towards the improvement of monitoring and data quality assessment in the weather radar network of the Meteorological Service of Catalonia. In 'Proceedings of the 8th European Conference on Radar in Meteorology and Hydrology (ERAD)', September 2014, Garmisch-Partenkirchen, Germany. (DLR)

Badia A, Saur´ı D, Cerdan R, Llurde´s JC (2002) Causality and management of forest fires in Mediterranean environments: An example from Catalonia. *Environmental Hazards* **4**, 23–32. doi:10.3763/EHAZ.2002.0403

Ballarotti MG, Saba MMF, Pinto O, Jr (2005) High-speed camera observations of negative ground flashes on a millisecond-scale. *Geophysical Research Letters* **32**, L23802. doi:10.1029/2005GL023889

Barnett K, Miller C, Venn TJ (2016) Using risk analysis to reveal opportunities for the management of unplanned ignitions in wilderness. *Journal of Forestry* **114**, 610–618. doi:10.5849/JOF.15-111

Bech J, Codina B, Lorente J, Bebbington D (2003) The sensitivity of single polarization weather radar beam blockage correction to variability in the

vertical refractivity gradient. *Journal of Atmospheric and Oceanic Technology* **20**(6), 845–855. doi:10.1175/1520-0426(2003)020,0845:TSOSPW.2.0.CO;2

Bech J, Vilaclara E, Pineda N, Rigo T, Lo´pez J, O'Hora F, Lorente J, Sempere D, Fa´bregas FX (2004) The weather radar network of the Catalan Meteorological Service: description and applications, In 'Proceedings of the European Conference on Radar in Meteorology and Hydrology (ERAD) 2004', Visby, Sweden. pp. 416–420. (Copernicus GmbH)

Brook M, Kitagawa N, Workman EJ (1962) Quantitative study of strokes and continuing currents in lightning discharges to ground. *Journal of Geophysical Research* **67**, 649–659. doi:10.1029/JZ067I002P00649

Brotons L, Aquilue N, de Caceres M, Fortin MJ, Fall A (2013) How fire history, fire suppression practices and climate change affect wildfire regimes in Mediterranean landscapes. *PLoS One* **8**, e62392. doi:10.1371/JOURNAL.PONE.0062392

Brown RA, Kaufman CA, MacGorman DR (2002) Cloud-to-ground lightning associated with the evolution of a multi-cell storm. *Journal of Geophysical Research* **107**, 4397. doi:10.1029/2001JD000968

Camia A, Durrant Houston T, San-Miguel J (2010) The European fire database: development, structure and implementation. In 'Proceedings of the VI International Conference on Forest Fire Research', 15–18 November 2010, Coimbra, Portugal. (Ed. DX Viegas) A20. (ADAI/CEIF, Coimbra, Portugal).

Campos LZS, Saba MMF, Pinto O, Jr, Ballarotti MG (2007) Waveshapes of continuing currents and properties of M-components in natural negative cloud-to-ground lightning from high-speed video observations. *Atmospheric Research* **84**, 302–310. doi:10.1016/J.ATMOSRES.2006.09.002

Carey LD, Rutledge SA (1996) A multiparameter radar case study of the microphysical and kinematic evolution of a lightning producing storm. *Meteorology and Atmospheric Physics* **59**, 33–64. doi:10.1007/BF01032000

Castellnou M, Miralles M (2010) The Catalonian program of fire management: GRAF team actions. In: 'Best practices of fire use. Prescribed burning and suppression fire programmes in selected case-study regions in Europe' EFI Research Report 24. (Eds C Montiel, D Kraus) pp. 137–152. (European Forest Institute)

Castellnou M, Kraus D, Miralles M (2010) Prescribed burning and suppression fire techniques: from fuel to landscape management, In: 'Best practices of fire use – Prescribed burning and suppression fire programmes in selected case-study regions in Europe' EFI Research Report 24. (Eds C Montiel, D Kraus) pp. 3–17. (European Forest Institute)

Cesti G, Conedera M, Spinedi F (2005) Considerazioni sugli incendi boschivi causati da fulmini. *Schweizerische Zeitschrift fu¨r Forstwesen* **156**, 353–361. doi:10.3188/SZF.2005.0353

Che`ze JL, Sauvageot H (1997) Area-average rainfall and lightning activity. *Journal of Geophysical Research* **102**, 1707–1715. doi:10.1029/96JD02972

Conedera M, Cesti G, Pezzatti GB, Zumbrunnen T, Spinedi F (2006) Lightning induced fires in the alpine region: an increasing problem. Presented at the V International Conference on Forest Fire Research. Coimbra, Portugal. pp. 9.

Costafreda-Aumedes S, Cardil A, Molina D, Daniel S, Mavsar R, Vega-Garcia C (2016) Analysis of factors influencing deployment of fire suppression resources in Spain using artificial neural networks. *iForest – Biogeosciences and Forestry* **9**, 138–145. doi:10.3832/IFOR1329-008

Cummins KL, Murphy MJ (2009) An overview of lightning locating systems: History, techniques, and data uses, with an in-depth look at the U.S. NLDN. *IEEE Transactions on Electromagnetic Compatibility* **51**(3), 499–518. doi:10.1109/TEMC.2009.2023450

Cummins KL, Murphy MJ, Bardo EA, Hiscox WL, Pyle RB, Pifer AE (1998) Acombined TOA/MDF technology upgrade of the U.S. national lightning detection network. *Journal of Geophysical Research* **103**, 9035–9044. doi:10.1029/98JD00153

Cummins KL, Cramer JA, Biagi CJ, Krider EP, Jerauld J, Uman MA, Rakov VA (2006) 6.1. The US National Lightning Detection Network: post-upgrade status. In 'Second Conference on Meteorological Applications of Lightning Data', January 2006, Atlanta, GA. (American Meteorological Society). Available at https://ams.confex.com/ams/Annual2006/techprogram/paper_105142.htm

Deierling W, Latham J, Petersen WA, Ellis SM, Christian HJ, Jr (2005) On the relationship of thunderstorm ice hydrometeor characteristics and total lightning measurements. *Atmospheric Research* **76**, 114–126. doi:10.1016/J.ATMOSRES.2004.11.023

del Moral A, Rigo T, Llasat MC (2018) A radar-based centroid tracking algorithm for severe weather surveillance: Identifying split/merge processes in convective systems. *Atmospheric Research* **213**, 110–120. doi:10.1016/J.ATMOSRES.2018.05.030

del Moral A, Weckwerth TM, Rigo T, Bell MM, Llasat MC (2020) C-Band dual-Doppler retrievals in complex terrain: improving the knowledge of severe storm dynamics in Catalonia. *Remote Sensing* **12**, 2930. doi:10.3390/RS12182930

Doswell CA, III (2001) Severe convective storms – an overview. In 'Severe Convective Storms'. Meteorological Monographs. (Ed CA Doswell) pp. 1–26. (American Meteorological Society: Boston, MA)

Dowdy AJ, Mills GA (2012) Atmospheric and fuel moisture characteristics associated with lightning-attributed fires. *Journal of Applied Meteorology and Climatology* **51**, 2025–2037. doi:10.1175/JAMC-D-11-0219.1

Duda JD, Gallus WA (2010) Spring and summer midwestern severe weather reports in supercells compared to other morphologies. *Weather and Forecasting* **25**, 190–206. doi:10.1175/2009WAF2222338.1

Duff TJ, Tolhurst KG (2015) Operational wildfire suppression modelling: a review evaluating development, state of the art and future directions. *International Journal of Wildland Fire* **24**, 735–748. doi:10.1071/WF15018

Duff TJ, Keane RE, Penman TD, Tolhurst KG (2017) Revisiting wildland fire fuel quantification methods: the challenge of understanding a dynamic, biotic entity. *Forests* **8**, 351. doi:10.3390/F8090351

Durden SL, Meagher JP, Haddad ZS (2004) Satellite observations of spatial and interannual variability of lightning and radar reflectivity. *Geophysical Research Letters* **31**, L18111. doi:10.1029/2004GL020384

Dye JE, Winn WP, Jones JJ, Breed DW (1989) The electrification of New Mexico thunderstorms: 1. Relationship between precipitation development and the onset of electrification. *Journal of Geophysical Research* **94**, 8643–8656. doi:10.1029/JD094ID06P08643

Evett RR, Mohrle CR, Hall BL, Brown TJ, Stephens SL (2008) The effect of monsoonal atmospheric moisture on lightning fire ignitions in southwestern North America. *Agricultural and Forest Meteorology* **148**, 1478–1487. doi:10.1016/J.AGRFORMET.2008.05.002

Fernandes PM, Santos JA, Castedo-Dorado F, Almeida R (2021) Fire from the sky in the Anthropocene. *Fire* **4**, 13. doi:10.3390/FIRE4010013

Flannigan MD, Wotton BM (1991) Lightning-ignited forest fires in northwestern Ontario. *Canadian Journal of Forest Research* **21**, 277–287. doi:10.1139/X91-035

Fuquay DM (1980) Lightning that ignites forest fires. In 'Proceedings of the Sixth Conference on Fire and Forest Meteorology'. 22–24 April 1980, Seattle, WA. (Eds RE Martin, *et al.*) pp. 109–112. (American Meteorological Society: Boston, MA)

Fuquay DM (1982) Positive cloud-to-ground lightning in summer thunderstorms. *Journal of Geophysical Research* **87**, 7131–7140. doi:10.1029/JC087IC09P07131

Fuquay DM, Baughman RG, Taylor AR, Hawe RG (1967) Characteristics of seven lightning discharges that caused forest fires. *Journal of Geophysical Research* **72**, 6371–6373. doi:10.1029/JZ072I024P06371

Gallus WA, Jr, Snook NA, Johnson EV (2008) Spring and summer severe weather reports over the Midwest as a function of convective mode: A preliminary study. *Weather and Forecasting* **23**, 101–113. doi:10.1175/2007WAF2006120.1

Ganteaume A, Camia A, Jappiot M, San Miguel-Ayanz J, Long-Fournel M, Lampin C (2013) A review of the main driving factors of forest fire ignition over Europe. *Environmental Management* **51**(3), 651–662. doi:10.1007/S00267-012-9961-Z

Gonza´lez JR, Pukkala T (2007) Characterization of forest fires in Catalonia (north-east Spain). *European Journal of Forest Research* **126**, 421–429. doi:10.1007/S10342-006-0164-0

Gracia C, Iba`n˜ez JJ, Burriel JA, Mata T, Vayreda J (2004) Inventari Ecolo`gic i Forestal de Catalunya. (CREAF – Centre de Recerca Ecolo`gica i Aplicacions Forestals: Barcelona) [In Catalan].

Granstro¨m A (1993) Spatial and temporal variation in lightning ignitions in Sweden. *Journal of Vegetation Science* **4**, 737–744. doi:10.2307/3235609

Greene DR, Clark RA (1972) Vertically Integrated Liquid water – a new analysis tool. *Monthly Weather Review* **100**, 548–552. doi:10.1175/1520-0493(1972)100,0548:VILWNA.2.3.CO;2

Hall BL (2007) Precipitation associated with lightning-ignited wildfires in Arizona and New Mexico. *International Journal of Wildland Fire* **16**, 242–254. doi:10.1071/WF06075

Hall BL (2008) Fire ignitions related to radar reflectivity patterns in Arizona and New Mexico. *International Journal of Wildland Fire* **17**, 317–327. doi:10.1071/WF06110

Hall BL, Brown TJ (2006) Climatology of positive polarity flashes and multiplicity and their relation to natural wildfire ignitions. In 'Proceedings of the 19th International Lightning Detection Conference', 24–27 April 2006, Tucson, AZ. Available at https://my.vaisala.net/Vaisala%20Documents/Scientific%20papers/Climatology_of_positive_polarity_flashes_and_multiplicity_and_their_relation_to_natural_wildfire_ignitions.pdf

Jain P, Wang X, Flannigan MD (2017) Trend analysis of fire season length and extreme fire weather in North America between 1979 and 2015. *International Journal of Wildland Fire* **26**, 1009–1020. doi:10.1071/WF17008

Johnson JT, MacKeen PL, Witt A, Mitchell EDW, Stumpf GJ, Eilts MD, Thomas KW (1998) The storm cell identification and tracking algorithm: an enhanced WSR-88D algorithm. *Weather and Forecasting* **13**, 263–276. doi:10.1175/1520-0434(1998)013,0263:TSCIAT.2.0.CO;2

Keeley JE, Syphard AD (2021) Large California wildfires: 2020 fires in historical context. *Fire Ecology* **17**. doi:10.1186/S42408-021-00110-7

Kera¨nen J (1929) Blitzschlag als Zu¨nder der Waldbrande im no¨rdlichen Finnland. *Forestalia Fennica Acta* **35**, 7238. doi:10.14214/AFF.7238 [in German]

Kitagawa N, Brook M, Workman EJ (1962) Continuing currents in cloud-to-ground lightning discharges. *Journal of Geophysical Research* **67**, 637–647. doi:10.1029/JZ067I002P00637

Kitterman CG (1980) Characteristics of lightning from frontal system thunderstorms. *Journal of Geophysical Research* **85**, 5503–5505. doi:10.1029/JC085IC10P05503

Komarek EV (1964) The natural history of lightning. In 'Proceedings Third Annual Tall Timbers Fire Eco1ogy Conference'. pp. 139–183. (Tall Timbers Research Station: Tallahassee, FL).

Krehbiel PR (1986) The electrical structure of thunderstorms. In 'The Earth's electrical environment'. pp. 90–113. (National Academies Press: Washington, DC)

Larjavaara M (2005) Climate and Forest Fires in Finland– Influence of Lightning-Caused Ignitions and Fuel Moisture. Doctoral Thesis. Department of Forest Ecology, Faculty of Agriculture and Forestry, University of Helsinki.

Larjavaara M, Pennanen J, Tuomi T (2005) Lightning that ignites forest fires in Finland. *Agricultural and Forest Meteorology* **132**, 171–180. doi:10.1016/J.AGRFORMET.2005.07.005

Latham D, Williams E (2001) Lightning and forest fires. In: 'Forest fires: Behavior and ecological effects'. (Eds EA Johnson, K Miyanishi) pp. 375–418. (Academic Press). doi:10.1016/B978-012386660-8/50013-1

Latham DJ, Schlieter JA (1989) Ignition probabilities of wildland fuels based on simulated lightning discharges. USDA Forest Service, Intermountain Research Station, Research Paper INT-411. (Ogden, UT, USA)

Liu C, Cecil DJ, Zipser EJ, Kronfeld K, Robertson R (2012) Relationships between lightning flash rates and radar reflectivity vertical structures in thunderstorms over the tropics and subtropics. *Journal of Geophysical Research* **117**, D06212. doi:10.1029/2011JD017123

Llasat MC, del Moral A, Corte`s M, Rigo T (2021) Convective precipitation trends in the Spanish Mediterranean region. *Atmospheric Research* **257**, 105581. doi:10.1016/J.ATMOSRES.2021.105581

Llasat-Botija M, Llasat MC, Lo´pez L (2007) Natural hazards and the press in the western Mediterranean region. *Advances in Geosciences* **12**, 81–85. doi:10.5194/ADGEO-12-81-2007

MacGorman DR, Rust WD, Williams ER (1999) The electrical nature of storms. *Physics Today* **52**. doi:10.1063/1.882670

MacGorman DR, Rust WD, Schuur TJ, Biggerstaff MI, Straka JM, Ziegler CL, Mansell ER, Bruning EC, Kuhlman KM, Lund NR, Biermann NS, Payne C, Carey LD, Krehbiel PR, Rison W, Eack KB, Beasley WH (2008) TELEX: The thunderstorm electrification and lightning experiment. *Bulletin of the American Meteorological Society* **89**, 997–1014. doi:10.1175/2007BAMS2352.1

MacNamara BR, Schultz CJ, Fuelberg HE (2020) Flash characteristics and precipitation metrics of western US lightning-initiated wildfires from 2017. *Fire* **3**, 5. doi:10.3390/FIRE3010005

March V, Montanya` J, Pineda N (2014) Negative lightning current parameters and detection efficiency for two operational LLS in Catalonia (NE Spain). In 'Proceedings of the International Conference on Lightning Protection (ICLP)', 2014, Shanghai, China. pp. 966–973. (IEEE). doi:10.1109/ICLP.2014.6973263

Mart´ın-Vide J, Brunet M, Prohom M, Rius A (2010) Els climes de Catalunya. Present i tende`ncies recents. In 'Segon informe sobre el canvi clima`tic a Catalunya', pp. 39–72. (Consell Assessor per al Desenvolupament Sostenible: Barcelona) [In Catalan]. Available at http://cads.gencat.cat/ca/publicacions/informes-sobre-el-canvi-climatic-a-catalunya/segon-informe-sobre-el-canvi-climatic-a-catalunya/

Matthews S (2014) Dead fuel moisture research: 1991–2012. *International Journal of Wildland Fire* **23**, 78–92. doi:10.1071/WF13005

Mazur V, Rust WD, Gerlach JC (1986) Evolution of lightning flash density and reflectivity structure in a multi-cell thunderstorm. *Journal of Geophysical Research* **91**, 8690–8700. doi:10.1029/JD091ID08P08690

McGuiney E, Shulski M, Wendler G (2005) Alaska lightning climatology and application to wildfire science. In 'Conference on Meteorological Applications of Lightning Data', 85th AMS Annual Meeting, San Diego, CA. American Meteorological Society. Available at https://ams.confex.com/ams/Annual2005/techprogram/paper_85059.htm

Meisner BN, Chase RA, McCutchan MH, Mees R, Benoit JW, Ly B, Albright D, Strauss D, Ferryman T (1993) Lightning fire ignition assessment model. In: 'Proceedings of the 12th International Conference on Fire and Forest Meteorology', 26–28 October 1993, Jekyll Island, GA. pp. 172–178. (Society of American Foresters, AMS: Boston, MA)

Metzger E, Nuss WA (2013) The relationship between total cloud lightning behaviour and radar-derived thunderstorm structure. *Weather and Forecasting* **28**(1), 237–253. doi:10.1175/WAF-D-11-00157.1

Minnich RA (1983) Fire mosaic in southern California and northern Baja California. *Science* **219**, 1287–1294. doi:10.1126/SCIENCE.219.4590.1287

Molinie G, Soula S, Chauzy S (1999) Cloud-to-ground lightning activity and radar observations of storms in the Pyrenees Range area. *Quarterly Journal of the Royal Meteorological Society* **125**, 3103–3122. doi:10.1256/SMSQJ.56014

Montanya` J, van der Velde OA, March V, Romero D, Sola` G, Pineda N (2012) High-speed video of lightning and X-ray pulses during the 2009–2010 observation campaigns in northeastern Spain. *Atmospheric Research* **117**, 91–98. doi:10.1016/J.ATMOSRES.2011.09.013

Morin AA, Albert-Green A, Woolford DG, Martell DL (2015) The use of survival analysis methods to model the control time of forest fires in Ontario. *Canadian Journal of Forest Research* **24**, 964–973.

Moris JV, Conedera M, Nisi L, Bernardi M, Cesti G, Pezzatti GB (2020) Lightning-caused fires in the Alps: Identifying the igniting strokes. *Agricultural and Forest Meteorology* **290**, 107990. doi:10.1016/J.AGRFORMET.2020.107990

Moritz MA, Batllori E, Bradstock RA, Gill AM, Handmer J, Hessburg PF, Leonard J, McCaffrey S, Odion DC, Schoennagel T, Syphard AD (2014) Learning to coexist with fire. *Nature* **515**, 58–66. doi:10.1038/NATURE13946

Mu¨ller MM, Vacik H (2017) Characteristics of lightnings igniting forest fires in Austria. *Agricultural and Forest Meteorology* **240–241**, 26–34. doi:10.1016/J.AGRFORMET.2017.03.020

Mu¨ller MM, Vacik H, Diendorfer G, Arpaci A, Formayer H, Gossow H (2013) Analysis of lightning-induced forest fires in Austria. *Theoretical and Applied Climatology* **111**, 183–193. doi:10.1007/S00704-012-0653-7

Murphy MJ, Cramer JA, Said RK (2021) Recent history of upgrades to the US National Lightning Detection Network. *Journal of Atmospheric and Oceanic Technology* **38**(3), 573–585. doi:10.1175/JTECH-D-19-0215.1

Nag A, Murphy MJ, Schulz W, Cummins KL (2015) Lightning locating systems: Insights on characteristics and validation techniques. *Earth and Space Science (Hoboken, N.J.)* **2**, 65–93. doi:10.1002/2014EA000051

Nauslar NJ, Kaplan ML, Wallmann J, Brown TJ (2013) A forecast procedure for dry thunderstorms. *Journal of Operational Meteorology* **1**(17), 200–214. doi:10.15191/NWAJOM.2013.0117

Nieto H, Aguado I, Garc´ıa M, Chuvieco E (2012) Lightning-caused fires in central Spain: development of a probability model of occurrence for two Spanish regions. *Agricultural and Forest Meteorology* **162–163**, 35–43. doi:10.1016/J.AGRFORMET.2012.04.002

Oliveras I, Gracia M, More´ G, Retana J (2009) Factors influencing the pattern of fire severities in a large wildfire under extreme meteorological conditions in the Mediterranean basin. *International Journal of Wildland Fire* **18**(7), 755–764. doi:10.1071/WF08070

Parker MD, Johnson RH (2000) Organizational modes of mid-latitude mesoscale convective systems. *Monthly Weather Review* **128**, 3413–3436. doi:10.1175/1520-0493(2001)129,3413:OMOMMC.2.0.CO;2

Petersen WA, Rutledge SA (1998) On the relationship between cloud-to-ground lightning and convective rainfall. *Journal of Geophysical Research* **103**, 14025–14040. doi:10.1029/97JD02064

Pezzatti GB, Zumbrunnen T, Bu¨rgi M, Ambrosetti P, Conedera M (2013) Fire regime shifts as a consequence of fire policy and socio-economic development: an analysis based on the change point approach. *Forest Policy and Economics* **29**, 7–18. doi:10.1016/J.FORPOL.2011.07.002

Pineda N, Montanya` J (2009) Lightning detection Spain: The particular case of Catalonia. In: 'Lightning: Principles, instruments and applications'. (Eds HD Betz, U Schumann, P Laroche) pp. 161–185. (Springer: the Netherlands)

Pineda N, Rigo T (2017) The rainfall factor in lightning-ignited wildfires in Catalonia. *Agricultural and Forest Meteorology* **239**, 249–263. doi:10.1016/J.AGRFORMET.2017.03.016

Pineda N, Rigo T, Bech J, Soler X (2007) Lightning and precipitation relationshipin summer thunderstorms: case studies in the north-western Mediterranean region. *Atmospheric Research* **85**, 159–170. doi:10.1016/J.ATMOSRES.2006.12.004

Pineda N, Montanya` J, van der Velde OA (2014) Characteristics of lightning related to wildfire ignitions in Catalonia. *Atmospheric Research* **135–136**, 380–387. doi:10.1016/J.ATMOSRES.2012.07.011

Plana E (2004) Incendis forestals, dimensio´ socioambiental, gestio´ del risc i ecologia del foc. Proccedings: Actes de les Jornades sobre Incendis Forestals i Recerca de la xarxa ALINFO. Xarxa ALINFO XCT2001–00061. Solsona, DL: L-501/2004. Centre Tecnolo`gic Forestal de Catalunya [In Catalan]

Pyne SJ, Andrews PL, Laven RD (1996) 'Introduction to wildland fire.' (John Wiley and Sons: New York)

Reid AM, Fuhlendorf SD, Weir JR (2010) Weather variables affecting Oklahoma wildfires. *Rangeland Ecology and Management* **63**, 599–603. doi:10.2111/REM-D-09-00132.1

Rigo T, Pineda N, Bech, J (2008) Estudi i modelitzacio´ del cicle de vida de les tempestes amb te`cniques de teledeteccio´. In 'Nota d'estudi del SMC (no. 72)'. pp. 23–44 (Generalitat de Catalunya: Barcelona) [In Catalan]

Rigo T, Pineda N, Bech J (2010) Analysis of warm season thunderstorms using an object-oriented tracking method based on radar and total lightning data. *Natural Hazards and Earth System Sciences* **10**, 1881–1893. doi:10.5194/NHESS-10-1881-2010

Riley KL, Thompson MP, Scott JH, Gilbertson-Day JW (2018) A model-based framework to evaluate alternative wildfire suppression strategies. *Resources* **7**(1), 4. doi:10.3390/RESOURCES7010004

Rodrigues M, Alcasena F, Vega-Garc´ıa C (2019) Modeling initial attack success of wildfire suppression in Catalonia, Spain. *The Science of the Total Environment* **666**. doi:10.1016/J.SCITOTENV.2019.02.323

Rodr´ıguez-Pe´rez JR, Ordo´n˜ez C, Roca-Pardin˜as J, Vec´ın-Arias D, Castedo-Dorado F (2020) Evaluating lightning-caused fire occurrence using spatial generalized additive models: A case study in central Spain. *Risk Analysis* **40**, 1418–1437. doi:10.1111/RISA.13488

Rorig ML, Ferguson SA (1999) Characteristics of lightning and wildland fire ignition in the Pacific Northwest. *Journal of Applied Meteorology* **38**, 1565–1575. doi:10.1175/1520-0450(1999)038,1565:COLAWF.2.0.CO;2

Rorig ML, Ferguson SA (2002) The 2000 Fire Season: Lightning-Caused Fires. *Journal of Applied Meteorology* **41**(7), 786–791. doi:10.1175/1520-0450(2002)041,0786:TFSLCF.2.0.CO;2

Rosenfeld D, Wolff DB, Atlas D (1993) General probability-matched relations between radar reflectivity and rain rate. *Journal of Applied Meteorology* **32**, 50–72. doi:10.1175/1520-0450(1993)032,0050:GPMRBR.2.0.CO;2

Rust WD, MacGorman DR, Taylor WL (1985) Photographic verification of continuing current in positive cloud-to-ground flashes. *Journal of Geophysical Research* **90**, 6144–6146. doi:10.1029/JD090ID04P06144

Saba MMF, Pinto O, Ballarotti MG (2006) Relation between lightning return stroke peak current and following continuing current. *Geophysical Research Letters* **33**, L23807. doi:10.1029/2006GL027455

Saba MMF, Schulz W, Warner TA, Campos LZS, Schumann C, Krider EP, Cummins KL, Orville RE (2010) High-speed video observations of positive lightning flashes to ground. *Journal of Geophysical Research* **115**, D24201. doi:10.1029/2010JD014330

Salvador A, Pineda N, Montanya` J, Sola` G (2020) Seasonal variations on the conditions required for the lightning production. *Atmospheric Research* **243**. doi:10.1016/J.ATMOSRES.2020.104981

Salvador A, Pineda N, Montanya` J, Lo´pez JA, Sola` G (2021) Thunderstorm charge structures favouring cloud-to-ground lightning. *Atmospheric Research* **257**, 105577. doi:10.1016/J.ATMOSRES.2021.105577

San-Miguel-Ayanz J, Moreno JM, Camia A (2013) Analysis of large fires in European Mediterranean landscapes: lessons learned and perspectives. *Forest Ecology and Management* **294**, 11–22. doi:10.1016/J.FORECO.2012.10.050

San-Miguel-Ayanz J, Durrant T, Boca R, Liberta` G, Branco A, de Rigo D, Ferrari D, Maianti P, Arte´s Vivancos T, Oom D, Pfeiffer H, Nuijten D, Leray T (2019) 'Forest fires in Europe, Middle East and North Africa 2018.' (Publications Office of the European Union: Luxembourg). doi:10.2760/1128

San Segundo H, Lo´pez JA, Pineda N, Altube P, Montanya` J (2020) Sensitivity analysis of lightning stroke-to-flash grouping criteria. *Atmospheric Research* **242**, 105023. doi:10.1016/J.ATMOSRES.2020.105023

Schultz CJ, Nauslar NJ, Wachter JB, Hain CR, Bell JR (2019) Spatial, temporal, and electrical characteristics of lightning in reported lightning-initiated wildfire events. *Fire* **2**, 18. doi:10.3390/FIRE2020018

Schulz W, Diendorfer G, Pedeboy S, Poelman DR (2016) The European lightning location system EUCLID – Part 1: Performance analysis and validation. *Natural Hazards and Earth System Sciences* **16**, 595–605. doi:10.5194/NHESS-16-595-2016

Shindo T, Uman MA (1989) Continuing current in negative cloud-to-ground lightning. *Journal of Geophysical Research* **94**, 5189–5198. doi:10.1029/JD094ID04P05189

Sopko P, Bradshaw L, Jolly M (2016) Spatial products available for identifying areas of likely wildfire ignitions using lightning location data – Wildand Fire Assessment System (WFAS). In 'Proceedings of the 6th International Lightning Meteorology Conference', San Diego, CA, USA, 18–21 April 2016. Available at https://my.vaisala.net/Vaisala%20Documents/Scientific%20papers/2016%20ILDC%20ILMC/Paul%20Sopko%20et%20al.%20Spatial%20Products%20Available%20for%20Identifying%20Areas%20of%20Likely%20Wildfire%20Ignitions.pdf

Sotillo MG, Ramis C, Romero R, Alonso S, Homar V (2003) Role of orography in the spatial distribution of precipitation over the Spanish Mediterranean zone. *Climate Research* **23**(3), 247–261. doi:10.3354/CR023247

Soula S, Chauzy S (2001) Some aspects of the correlation between lightning and rain activities in thunderstorms. *Atmospheric Research* **56**, 355–373. doi:10.1016/S0169-8095(00)00086-7

Steiger SM, Orville RE, Carey LD (2007) Total lightning signatures of thunderstorm intensity over north Texas. Part I: Supercells. *Monthly Weather Review* **135**, 3281–3302. doi:10.1175/MWR3472.1

Stocks BJ, Mason JA, Todd EM, Bosch BM, Wotton BD, Amiro MD, Flannigan KG, Hirsch KA, Logan DL, Martell DL, Skinner WR (2002) Large forest fires in Canada, 1959–1997. *Journal of Geophysical Research* **107**. doi:10.1029/2001JD000484

Stolzenburg M, Marshall TC (2008) Charge structure and dynamics in thunderstorms. *Space Science Reviews*. doi:10.1007/S11214-008-9338-Z

Takahashi T (1978) Riming electrification as a charge generation mechanism in thunderstorms. *Journal of the Atmospheric Sciences* **35**, 1536–1548. doi:10.1175/1520-0469(1978)035,1536:REAACG.2.0.CO;2

Tedim F, McCaffrey S, Leone V, Delogu GM, Castelnou M, McGee TK, Aranha J (2020) What can we do differently about the extreme wildfire problem: An overview. Chapter 13 in Extreme Wildfire Events and Disasters (Eds F Tedim, V Leone, TK McGee) pp. 233–263. (Elsevier). doi:10.1016/B978-0-12-815721-3.00013-8

Terradas J (1996) 'Ecologia del foc.' (Edicions Proa: Barcelona) [In Catalan].

Tessendorf SA, Rutledge SA, Wiens KC (2007) Radar and lightning observations of normal and inverted polarity multicellular storms from steps. *Monthly Weather Review* **135**(11), 3682–3706. doi:10.1175/2007MWR1954.1

Toracinta ER, Mohr KI, Zipser EJ, Orville RE (1996) A comparison of WSR-88D reflectivities, SSM/I brightness temperatures, and lightning for mesoscale convective systems in Texas. Part I: Radar reflectivity and lightning. *Journal of Applied Meteorology and Climatology* **35**(6), 902–918. doi:10.1175/1520-0450(1996)035,0902:ACOWRS.2.0.CO;2

Trapero L, Bech J, Rigo T, Pineda N, Forcadell D (2009) Uncertainty of precipitation estimates in convective events by the Meteorological Service of Catalonia radar network. *Atmospheric Research* **93**, 408–418. doi:10.1016/J.ATMOSRES.2009.01.021

van Wagtendonk JW, Lutz JA (2007) Fire Regime Attributes of Wildland Fires in Yosemite National Park, USA. *Fire Ecology* **3**, 34–52. doi:10.4996/FIREECOLOGY.0302034

Vant-Hull B, Thompson T, Koshak W (2018) Optimizing precipitation thresholds for best correlation between dry lightning and wildfires. *Journal of Geophysical Research, D, Atmospheres* **123**, 2628–2639. doi:10.1002/2017JD027639

Veraverbeke S, Rogers BM, Goulden ML, Jandt RR, Miller CE, Wiggins EB, Randerson JT (2017) Lightning as a major driver of recent large fire years in North American boreal forests. *Nature Climate Change* **7**, 529–534. doi:10.1038/NCLIMATE3329

Vincent BR, Carey L, Schneider D, Keeter K, Gonski R (2003) Using WSR-88D reflectivity data for the prediction of cloud-to-ground lightning: A North Carolina study. *National Weather Digest.* **27**, 35–44.

Westerling AL, Hidalgo HG, Cayan DR, Swetnam T (2006) Warming and earlier spring increase western US forest wildfire activity. *Science* **313**, 940–943. doi:10.1126/SCIENCE.1128834

Williams ER (1989) The tripole structure of thunderstorms. *Journal of Geophysical Research* **94**, 13151–13167. doi:10.1029/JD094ID11P13151

Williams ER, Weber ME, Orville RE (1989) The relationship between lightning type and convective state of thunderclouds. *Journal of Geophysical Research* **94**, 13213–13220. doi:10.1029/JD094ID11P13213

Williams ER, Zhang R, Rydock J (1991) Mixed-phase microphysics and cloud electrification. *Journal of the Atmospheric Sciences* **48**, 2195–2203. doi:10.1175/1520-0469(1991)048,2195:MPMACE.2.0.CO;2

Yang YH, King P (2010) Investigating the potential of using radar echo reflectivity to nowcast cloud-to-ground lightning initiation over southern Ontario. *Weather and Forecasting* **25**, 1235–1248. doi:10.1175/2010WAF2222387.1

Yuter SE, Houze RA (1995) Three-dimensional kinematic and microphysical evolution of Florida cumulonimbus. Part II: Frequency distributions of vertical velocity, reflectivity, and differential reflectivity. *Monthly Weather Review* **123**, 1941–1963. doi:10.1175/1520-0493(1995)123,1941:TDKAME.2.0.CO;2